Universidade do Minho
Escola de Medicina

Ana Margarida Machado Sousa

Unravelling the role of the spinocerebellar ataxia type 3-associated protein ATXN3 in glioblastoma

dezembro de 2021

Unravelling the role of the spinocerebellar ataxia type 3-associated protein ATXN3 in glioblastoma
Margarida Sousa
UMinho | 2021

Universidade do Minho
Escola de Medicina

Ana Margarida Machado Sousa

Unravelling the role of the spinocerebellar ataxia type 3-associated protein ATXN3 in glioblastoma

Dissertação de Mestrado
Mestrado em Ciências da Saúde

Trabalho efetuado sob a orientação da
Doutora Andreia Alexandra Neves de Carvalho
e da
Doutora Céline Saraiva Gonçalves

dezembro de 2021

AGRADECIMENTOS

Ao finalizar estes 2 anos de dedicação e trabalho, gostaria de expressar o meu agradecimento a todas as pessoas que me apoiaram e contribuíram para a realização deste trabalho.

Começo por agradecer às minhas orientadoras Doutora Andreia e Doutora Céline por me terem dado a oportunidade de aprender e evoluir como investigadora e por toda a disponibilidade e ensinamentos. Espero que este trabalho vos faça ficar orgulhosas. Agradeço também ao Doutor Bruno Costa e à Professora Patrícia Maciel por me terem dado a oportunidade de integrar os seus grupos de investigação. Obrigada também a todos os colegas de grupo e de laboratório. Em especial quero agradecer à Eduarda, pela disponibilidade, pela ajuda constante e crucial, pela paciência e pelos conhecimentos transmitidos. Foste, sem sombra de dúvidas, uma grande ajuda neste ano. Agradeço também à Liliana e à Doutora Sara Silva, que tiveram também um papel importante na minha aprendizagem, por estarem sempre disponíveis para me ajudarem e tirarem dúvidas sempre que possível. Estou-vos grata!

Agradeço aos meus colegas de mestrado, em especial à Adriana, Marcela, Beatriz e Joana por todas as palavras de conforto quando necessitei e por estarem sempre disponíveis. A todos os meus amigos, especialmente ao Cenas, por todos as conversas aleatórias, por todo o apoio nos maus momentos e por estarem sempre lá.

Por último, gostaria de agradecer à minha família (a melhor do mundo) e sobretudo aos meus pais e ao Rúben, pelo amor, por me apoiarem incondicionalmente, pela força a continuar e por acreditarem sempre em mim, muitas das vezes mais do que eu própria. Não há palavras para exprimir tudo o que sinto. Sem vocês nada disto seria possível, devo-vos tudo!

FUNDING

The work presented in this thesis was performed in the Life and Health Sciences Research Institute (ICVS), University of Minho. Financial support was provided by Fundação Calouste Gulbenkian and Liga Portuguesa Contra o Cancro (to Bruno M. Costa); by grants from the ICVS Scientific Microscopy Platform, member of the national infrastructure PPBI - Portuguese Platform of Bioimaging (PPBI-POCI-01-0145-FEDER-022122; by the project NORTE-01-0145-FEDER-000055, supported by Norte Portugal Regional Operational Programme (NORTE 2020), under the PORTUGAL 2020 Partnership Agreement, through the European Regional Development Fund (ERDF) and by National funds, through the Foundation for Science and Technology (FCT) - project UIDB/50026/2020 and UIDP/50026/2020.

STATEMENT OF INTEGRITY

I hereby declare having conducted this academic work with integrity. I confirm that I have not used plagiarism or any form of undue use of information or falsification of results along the process leading to its elaboration.

I further declare that I have fully acknowledged the Code of Ethical Conduct of the University of Minho.

RESUMO

Desvendando o papel da proteína associada à ataxia espinocerebelosa tipo 3 ATXN3 em glioblastoma

O glioblastoma (GBM) é o tipo de glioma mais comum e maligno em adultos. Apesar dos esforços para investigar diversos tratamentos, os pacientes com GBM apresentam uma evolução clínica rápida e desfavorável, com uma sobrevida mediana de apenas 15 meses após o diagnóstico. Para além disso, a elevada atividade proliferativa e a natureza heterogénea e complexa do GBM estão associadas a um resultado clínico imprevisível e diverso. Assim, a identificação de marcadores moleculares de prognóstico que permitam a categorização de subgrupos de pacientes com GBM é fundamental para contribuir para a melhoria do seu resultado clínico. A ataxina-3 (ATXN3), a proteína envolvida na doença neurodegenerativa Ataxia espinocerebelosa tipo 3 (SCA3), é uma proteína conservada evolutivamente e expressa de forma ubíqua, que foi proposta como sendo uma enzima desubiquitinase. Além do seu envolvimento em SCA3, foi sugerido que a ATXN3 desempenha um papel em cancro, desempenhando funções oncogénicas ou supressoras tumorais dependendo do tipo tumoral. Uma vez que nenhum estudo, até ao momento, explorou o potencial envolvimento da ATXN3 em gliomas, e, particularmente em GBM, neste trabalho pretendemos, pela primeira vez, avaliar o papel funcional da ATXN3 em GBM e a sua relevância clínica nesta doença.

Observámos que a expressão da *ATXN3* diminui significativamente nos graus mais elevados de glioma, sendo menos expressa em GBM quando comparada com gliomas de baixo grau. Adicionalmente demonstrámos que a expressão da *ATXN3* está associada à mutação de IDH e à codeleção 1p/19q. Em células de GBM, observámos que a ATXN3 é expressa em todos os modelos testados, ao nível de RNAm e ao nível da proteína. Funcionalmente, a sobre-expressão da ATXN3 foi associada a uma diminuição significativa da viabilidade celular e da invasão em modelos *in vitro* de GBM. No entanto, em relação à proliferação e à migração celular não foi detetado um efeito estatisticamente significativo nos mesmos modelos. Estes dados sugerem que a ATXN3 pode ter funções de gene supressor tumoral em GBM, diminuindo a agressividade destes gliomas *in vitro*. Em pacientes com GBM, descobrimos que a ATXN3 tem valor de prognóstico clínico, estando associada a uma sobrevida global mais longa, independentemente de outros potenciais fatores de prognóstico.

Em suma, este trabalho permitiu que se compreendesse o papel da ATXN3 em GBM ao identificá-la como um gene supressor tumoral, e como um novo biomarcador de prognóstico favorável, trazendo novos conhecimentos sobre os mecanismos moleculares subjacentes a esta doença mortal.

Palavras-chave: Ataxina-3; Biomarcador de Prognóstico; Gene Supressor Tumoral; Glioblastoma; Glioma

ABSTRACT

Unravelling the role of the spinocerebellar ataxia type 3-associated protein ATXN3 in glioblastoma

Glioblastoma (GBM) is the most common and malignant type of glioma in adults. Despite the efforts to investigate various treatments, GBM patients exhibit a rapid and unfavorable clinical evolution, with a median overall survival of only 15 months after diagnosis. Furthermore, the high proliferative activity, and heterogeneous and complex nature of GBM is associated with an unpredictable and distinct clinical outcome. Thus, the identification of molecular prognostic markers that allow the categorization of subgroups of patients with GBM is critical to contribute to the improvement of their clinical outcome. Ataxin-3 (ATXN3), the protein involved in the neurodegenerative disease Spinocerebellar Ataxia Type 3 (SCA3), is an evolutionarily conserved and ubiquitously expressed protein, which has been proposed to act as a deubiquitinating enzyme. In addition to its involvement in SCA3, ATXN3 was suggested to play a role in cancer, performing oncogenic or tumor suppressive functions depending on the tumor type. Since no study to date has explored the potential involvement of ATXN3 in gliomas, and particularly in GBM, in this work we intend, for the first time, to evaluate the functional role of ATXN3 in GBM and the clinical relevance of this protein in this deadly disease.

We observed that *ATXN3* expression decreases significantly with glioma grade, being less expressed in GBM when compared to lower-grade gliomas, and that it is associated with IDH mutation and 1p/19q codeletion. Specifically in GBM cells, we observed that ATXN3 is expressed in all cell models tested, both at the mRNA and protein level. Functionally, ATXN3 overexpression was associated with a significant decrease in the cell viability and invasion of GBM *in vitro* models, although no statistically significant effect was observed regarding cell proliferation and migration. This data suggests that ATXN3 may have tumor suppressive functions in GBM, decreasing its aggressiveness *in vitro*. In GBM patients, we found that *ATXN3* has clinical prognostic value, being associated with longer overall survival, independently of other potential prognostic factors.

In summary, this work allowed the understanding of the role of ATXN3 in GBM by identifying it as a tumor suppressor gene, and as a new prognostic biomarker of favorable outcome, bringing new knowledge about the molecular mechanisms underlying this deadly disease.

Keywords: Ataxin-3, Glioblastoma, Glioma, Prognostic biomarker, Tumor suppressor gene

CONTENTS

ABBREVIATIONS

Akt	v-Akt Murine Thymoma viral oncogene homolog
ANOVA	Analysis of Variance
ATCC	American Type Culture Collection
ATXN3	Ataxin-3
BBB	Brain Blood Barrier
BrdU	Bromodeoxyuridine
CAG	Cytosine-Adenine-Guanine (Trinucleotide codon encoding glutamine)
CI	Confidence interval
cDNA	Complementary DNA
CNS	Central nervous system
CNV	Copy number variations
CO_2	Carbon Dioxide
DAPI	4',6-diamidino-2-phenylindole
DMEM	Dulbecco's Modified Eagle Medium
DMSO	Dimethyl Sulfoxide
DNA	Deoxyribonucleic Acid
DTT	Dithiothreitol
DUB	Deubiquitinating enzyme
ECL	Enhanced ChemiLuminescence
E. coli	*Escherichia coli*
EDTA	Ethylenediamine tetraacetic acid
EGF	Epidermal growth factor
ELISA	Enzyme-linked immunosorbent assay
FBS	Fetal Bovine Serum
GAPDH	Glyceraldehyde 3-phosphate dehydrogenase
GBM	Glioblastoma
HCl	Hydrochloric Acid
HGG	Higher-Grade Gliomas
HPRT1	hypoxanthine phosphoribosyltransferase 1
HR	Hazard ratios
IDH	Isocitrate dehydrogenase

JD	Josephin domain
KLF4	Krüppel-like factor 4
KPS	Karnofsky Performance Status
LB	Luria Bertani
LGG	Lower-Grade Gliomas
MGMT	O^6 methylguanine-DNA methyltransferase
mRNA	Messenger RNA
MTS	(3-(4,5-Dimethylthiazol-2-yl)-5-(3-carboxymethoxyphenyl)-2-(4-sulfophenyl)-2H-tetrazolium)
NaCl	Sodium Chloride
NADPH	Nicotinamide adenine dinucleotide phosphate
NES	Nuclear export signals
NLS	Nuclear Localization Signal
OS	Overall Survival
OSCC	Oral squamous cell carcinoma
PBS	Phosphate Buffered Saline
PCR	Polymerase Chain Reaction
PI	Propidium iodide
polyQ	Polyglutamine
PTEN	Phosphatase and tensin homolog
qPCR	Quantitative PCR
qRT-PCR	Quantitative Reverse Transcription-PCR
RIPA	Radioimmunoprecipitation assay buffer
RNA	Ribonucleic Acid
RT	Room Temperature
SCA3	Spinocerebellar Ataxia Type 3
SD	Standard Deviation
SDS	Sodium Dodecyl Sulfate
TAE	Tris-acetate-EDTA buffer
TBE	Tris-borate-EDTA buffer
TCGA	The Cancer Genome Atlas
TMZ	Temozolomide

UIM	Ubiquitin-interacting motifs
Ub	Ubiquitin
UPS	Ubiquitin-proteasome system
WB	Western Blot
WHO	World Health Organization

FIGURE LIST

TABLE LIST

1. | INTRODUCTION

1. INTRODUCTION

1.1 Cancer Overview

Cancer is a multifaceted public health problem and the second most common cause of death around the world (Bray et al., 2021), despite the efforts observed over the past few decades to improve different potential treatments. A staggering number of people are affected by cancer – according to the World Health Organization (WHO), it is estimated that about 19.3 million of new cancer cases were diagnosed and 9.96 million cancer deaths were accounted in 2020 worldwide (Ferlay, Ervik, et al., 2020; Sung et al., 2021). The cancer burden is projected to increase, with a predicted 24.6 million new cancer cases and 12.9 million cancer-related deaths occurring annually by 2030 (Ferlay, Laversanne, et al., 2020), a consequence of population growth and aging (Fidler et al., 2018).

Cancer is usually a disease associated with rapid proliferation and uncontrolled cell growth. However, the development of malignancy is a much more complex and highly dynamic process, involving multiple steps (Grizzi & Chiriva-Internati, 2006). Different types of normal cells progressively evolve into a malignant state through the acquisition of multiple biological characteristics (**Figure 1**). These distinct cells participate in heterotypic interactions with one another forming a complex tissue, called a tumor. These biological characteristics, responsible for the malignancy of the tumor, are designated "hallmarks of cancer" and were proposed by Hanahan & Weinberg, 2011: (i) evading growth suppressors, (ii) avoiding immune destruction, (iii) enabling replicative immortality, (iv) tumor-promotion inflammation, (v) activating invasion and metastasis, (vi) inducting angiogenesis, (vii) genome instability and mutation, (viii) resisting cell death, (ix) deregulating cellular energetics, and (x) sustaining proliferative signaling.

The evolution of these alterations leading to tumor progression and associated heterogeneity involves the gradual accumulation of genetic and epigenetic cancer-promoting changes, affecting many of the cell's regulatory mechanisms and functions – DNA mutations, copy number variations (CNV - deletions and amplifications), chromosomal rearrangements (deletions, inversions and translocation) and epigenetic modifications (DNA methylation and histone modifications) (Brait & Sidransky, 2011; Hanahan & Weinberg, 2011). Generally, these genetic and epigenetic alterations lead to the activation of oncogenes and inactivation of tumor suppressor genes (Vogelstein & Kinzler, 2004).

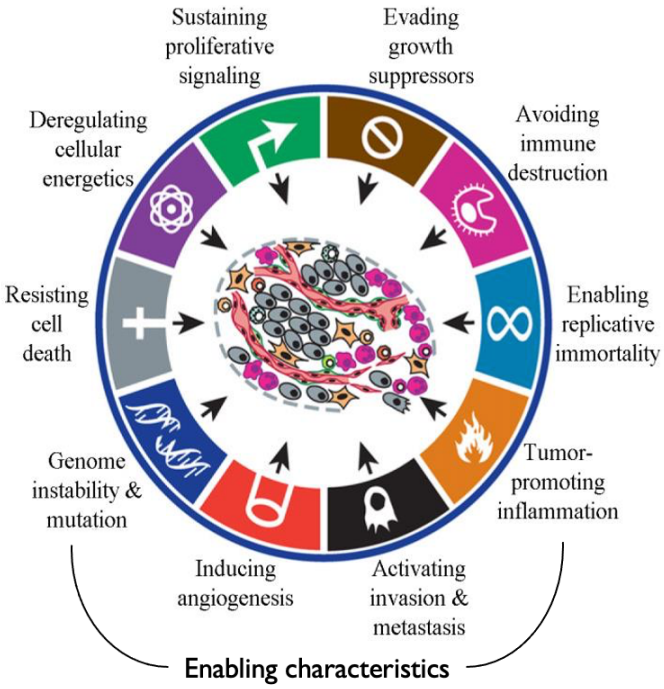

Figure 1. The eight hallmarks and two enabling characteristics of cancer proposed by Hanahan and Weinberg. Cancer cells present biological characteristics that contribute to tumor growth and progression (Adapted from Hanahan & Weinberg, 2011).

1.2 Primary Brain Tumors

Primary brain tumors originate from abnormal brain cells, in contrast to metastatic brain tumors that appear elsewhere in the body and spread to the brain region, usually through the bloodstream (Fayed, 2020). Despite their low incidence, accounting only for approximately 2% of all cancers, primary brain tumors have a high morbidity and mortality rate (Buckner et al., 2007). Furthermore, they rank first regarding average of years of life lost among all tumor types (Burnet et al., 2005), and are also the leading cause of cancer-related death in people under 40 in Europe (Ferlay, Ervik, et al., 2020). Indeed, these types of tumors are one of the most feared forms of cancer not only because of their poor prognosis, but also because of the direct repercussions on patients' quality of life and cognitive function. According to WHO, in 2020 the world estimated incidence of brain and nervous system tumors was approximately 308000 new cases, being the 19th most common cancer type. Regarding mortality, in the same year, approximately 251300 deaths were estimated worldwide, being the 12th most deadly cancer type. In Portugal, 1105 new cases and 933 deaths were reported in 2020 (Ferlay, Ervik, et al., 2020).

Geographically, Northern Europe, the USA white population and Israel are the regions that have the highest rates of reported cases and death due to primary malignant brain tumors (11-20 per 100000 inhabitants), while India and the Philippines have the lowest rates (2–4 per 100,000 inhabitants) (Ostrom et al., 2017; Walsh et al., 2016). However, these differences in brain tumors' incidence by geographic

region are frequently due to worldwide differences in medical care access and diagnostic impossibility (Ostrom et al., 2017).

1.3 Glioma

Glioma is the most common type of malignant brain tumor, accounting for about 80% of all primary malignant brain tumors, and is characterized by being heterogeneous and frequently lethal (Ostrom et al., 2020). Gliomas are divided into diffuse and circumscribed gliomas; however, the latter are not the focus of this dissertation and will not be explored. Since 2016, according to the WHO, tumors of the central nervous system (CNS) are classified according to their localization, morphological similarities with different types of neuroglial cells (histologic features), molecular parameters and grades of malignant behavior (**Figure 2**). This recent classification was a step forward in improving the molecular characterization of gliomas, highlighting key molecular alterations such as isocitrate dehydrogenase (IDH) mutation and 1p/19q codeletion (Louis et al., 2016). This approach combining histological and molecular classifications results in greater clinical/diagnostic accuracy and a better determination of therapeutic strategies, which reflects in better patient management.

IDH mutations

The finding of somatic mutations in the *IDH1* and *IDH2* genes, in a subgroup of glioblastomas (GBM), in genomic studies conducted by Parsons et al. in 2008 was perhaps the most important breakthrough in the molecular understanding and diagnosis of gliomas (Parsons et al., 2008).

IDH is an NADP+-dependent enzyme that catalyzes the oxidative decarboxylation of isocitrate to α-ketoglutarate with simultaneous production of NADPH (Reitman & Yan, 2010). The mutation affects the amino acid arginine at position 132 – critical for isocitrate binding – which is usually replaced by histidine (R132H) (Yan et al., 2009). This mutation causes the active site residues to be shifted, resulting in structural alterations that prevent IDH from performing its usual enzymatic function. As a result, the mutant IDH enzyme has the ability to convert α-ketoglutarate to R-2-hydroxyglutarate, excessive accumulation of which contributes to tumorigenesis (Dang et al., 2009). IDH mutations are highly frequent in WHO grade II and III gliomas (60-90%), but rarely occur in GBM (5-10%) (Cohen et al., 2013; Turkalp et al., 2014). Furthermore, IDH mutations occur mainly in younger patients and predict longer patient survival. In fact, GBM patients presenting IDH mutation have a median overall survival (OS) of 31 months, compared to 15 months for patients who did not have the mutation (Yan et al., 2009).

1p/19q codeletion

The 1p/19q codeletion is an event of genetic loss, being associated with tumors of the oligodendroglial lineage. It is estimated that 80-90% of grade II oligodendrogliomas and 50-70% of grade III oligodendrogliomas have the 1p/19q codeletion (Cairncross & Jenkins, 2008; Jansen et al., 2010). The 1p/19q codeletion involves the deletion of the short arm of chromosome 1 and the deletion of the long arm of chromosome 19, resulting in an unbalanced translocation involving the centromeric regions (Jenkins et al., 2006). So far, the role this codeletion plays in carcinogenesis is not clear. However, patients with this genetic event have been shown to have a significantly better OS and prognosis (J. S. Smith et al., 2000).

Histologically, gliomas are divided, based on microscopic similarities with glial cells of origin, in astrocytomas and oligodendrogliomas (Louis et al., 2016, 2021). Furthermore, considering the WHO classification, gliomas are grouped into four grades (I to IV) according to the histological presence/absence of cytological atypia, anaplasia, mitotic activity, microvascular proliferation, and necrosis. Grade I gliomas are considered benign, have low proliferative potential and well-differentiated cells. Grade II gliomas, despite having low aggressiveness, are classified as malignant tumors since they have diffuse infiltration capacity, which makes surgical removal of the tumor difficult. Grade III gliomas are characterized by a higher cellular density and present evidence of malignancy, such as nuclear atypia and high mitotic activity. Grade II and III gliomas tend to progress to higher-grade gliomas (HGG). Finally, grade IV gliomas represent the most malignant glioma, exhibit vascular proliferation and necrosis, and present a rapid progression of the disease with a lethal outcome, despite aggressive multimodal treatment (Louis et al., 2007; Riemenschneider & Reifenberger, 2009; Svien & Mabon, 1949; Weller et al., 2015).

Thus, gliomas include (i) astrocytomas (grade II and III), IDH-mutant or IDH-wildtype; (ii) oligodendrogliomas (grade II and III), IDH-mutant, 1p/19q codeleted; and (iii) GBM (grade IV), IDH-mutant or IDH-wildtype (**Figure 2**) (Louis et al., 2016). In 2021, this classification was updated, emphasizing the role of molecular diagnosis. The major alteration for the glioma classification is that GBM IDH-mutant tumors are now classified as astrocytoma, IDH-mutant grade IV (Louis et al., 2021).

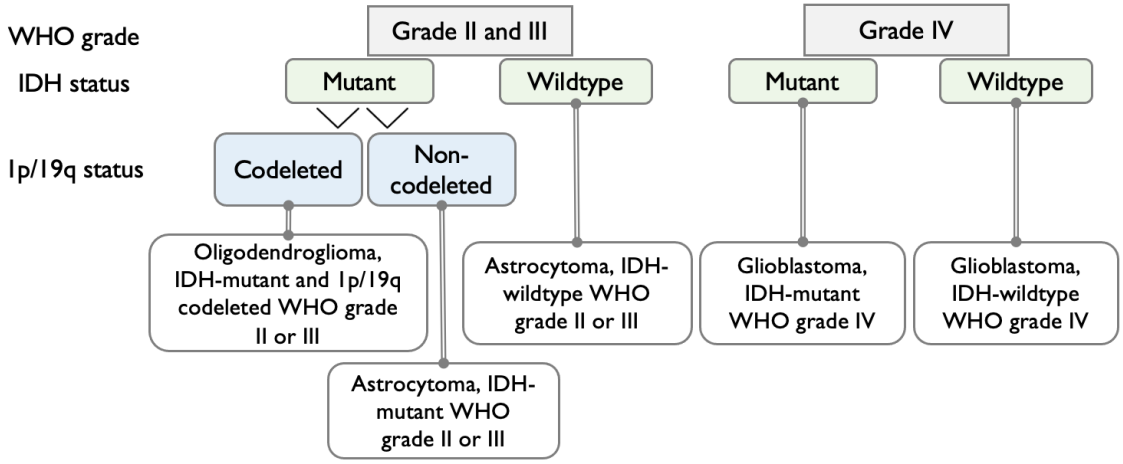

Figure 2. Classification of diffuse gliomas according to the 2016 WHO classification of CNS tumors. In addition to the morphological appearances already defined and the location of the tumor, the 2016 classification began to include important molecular alterations such as the IDH mutation and the 1p/19q codeletion status.

Efforts to establish possible glioma predisposition risk factors have been made. However, most of the results were inconsistent and a definitive link is yet to be discovered. In terms of environmental risk factors, ionizing radiation (exposure to therapeutic or diagnostic doses, or high-dose radiation) is the only linked to an increased risk of brain tumors, more specifically, glioma (Braganza et al., 2012; Elsamadicy et al., 2015; Preston et al., 2007). Indeed, different studies have shown that survivors of atomic bomb explosions in Nagasaki and Hiroshima exposed to high doses radiation have an increased incidence rate of brain tumors, including gliomas (Preston et al., 2007). Additionally, it has been reported that the therapeutic use of ionizing radiation to treat *Tinea capitis* and skin hemangioma in children and infants is associated with an increased relative risk of developing glioma (Sadetzki et al., 2005). Other studies have evaluated the potential effect of diet (Chen et al., 2002; Qin et al., 2014), smoking (Shao et al., 2016), electromagnetic fields (Coble et al., 2009), cell phone exposure (Ahlbom et al., 2009; Benson et al., 2013), among other factors, on the risk of glioma incidence. However, the results were inconsistent, and no conclusive correlation was observed. Growing evidence has shown that patients with allergies or autoimmune diseases are linked to a lower risk of glioma (Schoemaker et al., 2006; Schwartzbaum et al., 2012; Wiemels et al., 2002).

1.4 Glioblastoma (GBM)

Glioblastoma (GBM), classified by the WHO as grade IV, is the most common and malignant type of glioma in adults, accounting for more than 50% of all gliomas, and with a global annual incidence rate of 3.23 per 100000 population (Ostrom et al., 2020). Under standard-of-care treatment these patients present a median survival of approximately 15 months after diagnosis (Stupp et al., 2005). Although

GBMs can occur in all age groups, the incidence peak usually occurs between 45 and 70 years. Males are more affected than females (1.6:1) and Whites more than Blacks (2:1) (Walsh et al., 2016).

Histologically, GBM presents cellular polymorphism, nuclear atypia, frequent mitotic activity, vascular thrombosis, microvascular proliferation in the tumor margin and necrosis observed in the central portion of the tumor. The tumor mass is characterized by extensive heterogeneity at the cellular and molecular level and a weak delimitation without capsule, which makes GBMs highly aggressive, infiltrating and diffuse (So et al., 2021) These characteristics result in an extensive spread of tumor cells within the brain, which makes complete surgical resection difficult and recurrences almost certain (Brandes et al., 2008; Louis et al., 2007; C. Smith & Ironside, 2007; Weller et al., 2015).

As previously mentioned, in the 2016 WHO classification, GBM were subdivided into two subtypes, taking into account the status of IDH mutation: (i) GBM, IDH-wildtype and (ii) GBM, IDH-mutant (Louis et al., 2016). IDH-wildtype GBMs are the most common, accounting for approximately 90% of cases, and appear as a *de novo* process, that is, without pre-existing clinical or histological evidence of a lower-grade precursor. These tumors tend to be very aggressive and to develop quickly, occurring preferentially in elderly patients (incidence peak is 62 years) (Masui et al., 2016; Ohgaki & Kleihues, 2013). In contrast, IDH-mutant GBMs develop progressively from a pre-existing diffuse or anaplastic astrocytoma, generally over a period of 5 to 10 years. The incidence peak occurs in younger patients, around 44 years old, and they have a better prognosis (Louis et al., 2016; Ohgaki & Kleihues, 2013). The molecular profile of these tumors is similar to that of IDH-mutant astrocytomas (Masui et al., 2016). As a result, in the new 2021 classification of CNS tumors, GBM IDH-mutant were categorized as astrocytomas, IDH-mutant, grade IV. Thus, GBM IDH-wildtype became the unique type of GBM (Louis et al., 2021).

GBMs occur exclusively in the brain and are commonly located in the supratentorial region, occurring in the four lobes: frontal (26.8%), temporal (20.2%), parietal (11.6%) and occipital (2.8%). However, although relatively rare, GBMs can also appear in the brainstem (4.3%) and cerebellum (2.8%). (Ostrom et al., 2020). These tumors are highly infiltrating, and approximately half infiltrate more than one lobe and approximately 5% grow multifocally, in adults (Djalilian et al., 1999; Wirsching et al., 2016). The clinical outcome of GBM patients has been demonstrated to be influenced by tumor site. Indeed, a study demonstrated that patients with frontal lobe GBM had a longer survival compared to patients with temporal or parietal lobe GBM (11.4 months *vs*. 9.1 and 9.6 months, respectively) (Simpson et al., 1993). While GBM metastases to distant organs are extremely rare, metastases to bones, lungs, pleura, liver, mesentery, lymph nodes, liver and neck have been reported (Cunha & Maldaun, 2019; Pasquier et al., 1980; Rosen et al., 2018; Schweitzer et al., 2001; Seo et al., 2012).

Depending on the size and location of the tumor, the clinical presentation of a patient with a newly diagnosed GBM can vary widely. The increased intracranial pressure, which is a consequence of the gradual increase in tumor size and the edema surrounding the tumor, often causes headache and focal or progressive neurological deficits. Seizures manifest in about 20% to 40% of patients and gait imbalance and incontinence can also be manifested, usually in larger tumors. Non-specific complaints include headaches, dizziness, nausea, lethargy, hemiparesis, visual loss, speech difficulties, stroke-like symptoms, memory problems or personality changes, the last often confused with psychiatric disorders or dementia, especially in the elderly individuals (Hanif et al., 2017; Iacob & Dinca, 2009; Omuro & DeAngelis, 2013).

1.4.1 GBM Treatment: a multimodal approach

Despite the efforts to investigate different successful treatments and recent advances in the understanding of GBM molecular mechanisms, effectively treating GBM patients presenting a rapid and unfavorable clinical evolution remains difficult. GBM has an unpredictable response to most therapies mainly because of its high proliferative activity, infiltration of surrounding tissues, and heterogeneous and complex nature. In addition, the blood-brain barrier (BBB) makes treatment even more difficult as it limits the effectiveness of targeted-site therapies (Iacob & Dinca, 2009; Taylor et al., 2019).

A multimodal approach is needed for the treatment of GBM. The current standard therapy is based on maximal surgical resection, followed by radiotherapy and chemotherapy with administration of alkylating agent (Clarke et al., 2010; Stupp et al., 2005, 2006, 2009; Wilson et al., 2014). Surgical resection is performed with maximum safety in order to reduce the tumor load and avoid putting the patient's neurological function at risk (Lukas et al., 2019). However, owing to the invasive nature of GBM, this therapy is not curative and rarely eliminates residual tumor cells which may lead to disease progression or recurrence in the future (Brandes et al., 2008; Lukas et al., 2019). Thus, post-surgical treatment – concomitant and adjuvant radiotherapy and chemotherapy with alkylating agent – is needed to prevent recurrence (Hanif et al., 2017; Lukas et al., 2019). The alkylating agents cause DNA damage and selective cytotoxicity, which leads to apoptosis and cell death, by adding methyl groups at different positions in the DNA (Strobel et al., 2019). Several alkylating agents have been tested for their effectiveness in treating GBM, with temozolomide (TMZ) emerging as the gold standard chemotherapeutic agent (Stupp et al., 2005). TMZ acts by adding a methyl group at the N7 position of guanine, O3 position of adenine and O6 position of guanine. Alkylation of the O6 site on guanine is the main reason that leads to a cytotoxic effect in tumor cells, resulting in double-strand breaks and base mispairing in DNA, resulting in cell cycle arrest and apoptosis (Strobel et al., 2019; J. Zhang et al., 2012). TMZ was discovered in the

1970s and approved by the Food and Drug Administration in 2005 after a large international clinical trial by Stupp et al. have demonstrated that TMZ administration resulted in prolonged survival of GBM patients. This study showed that when patients were treated with concomitant and adjuvant radiotherapy with TMZ compared to radiotherapy alone, their OS improved by 2.5 months (12.1 months *vs* 14.6 months) (Stupp et al., 2005). Moreover, TMZ is able to cross the BBB and to reach therapeutically relevant concentrations in the brain (Strobel et al., 2019; Taylor et al., 2019). Thus, the standard of care for the treatment of GBM consists of postoperative radiotherapy (a total of 60 Gy in 30 fractions – 2 Gy per daily fraction) with concomitant daily TMZ administration, followed by 6 cycles of adjuvant TMZ (Stupp et al., 2005, 2009; Wilson et al., 2014).

1.4.2 Molecular prognostic factors of GBMs

Unfortunately, the standard therapy currently available for GBM patients is unable to change the lethality of this disease. Furthermore, the molecular and genetic heterogeneity of GBMs contributes to a varied response to treatments. Thus, the identification of molecular markers of prognosis allowing the categorization of subgroups of GBM patients is critical to improve their treatment outcomes and attempting to personalize their clinical management. Patient's age, Karnofsky performance status (KPS), and surgical resection's extent are the most consistent and well-established prognostic variables in GBM. Patient's age is a predictor of poor prognosis, as older patients tend to present a shorter OS than younger patients. Furthermore, patients with a higher KPS have a longer OS. Also, more complete resections are associated with better OS results (Ahmadloo et al., 2013; Xavier-Magalhães et al., 2013). Mutations in the *IDH* gene (formerly mentioned) (Cohen et al., 2013) and the methylation of the O-6-methylguanine-DNA methyltransferase (*MGMT*) gene promoter (Hegi et al., 2004) are the only ones currently being used in the clinical context for GBM patient stratification.

MGMT promoter methylation status

The most promising biomarker for response to therapy so far is, undoubtedly, the promoter methylation of the *MGMT* gene. This gene encodes a ubiquitously expressed DNA repair enzyme that removes alkyl groups from the O6 position of guanine (Wick et al., 2014). This DNA alkylation site is the target of the TMZ alkylating agent in treating tumor cells (Strobel et al., 2019). Thus, the activity of the MGMT enzyme interferes with the effect of TMZ, counteracting its therapeutic efficacy, which represents a potential mechanism of resistance to therapy (Feldheim et al., 2019; Wick et al., 2014). Hypermethylation of the *MGMT* promoter results in its epigenetic silencing, thus inducing loss of

expression. Consequently, DNA repair activity is reduced leading to increased sensitivity to alkylating agents (Esteller et al., 2000). Of note, *MGMT* expression is reduced in around 50% of GBMs. Studies have shown that this silencing of the *MGMT* promoter region is associated with a higher OS of GBM patients. Indeed, Hegi and colleagues observed that the median survival was 21.7 months for patients whose tumor contained the methylated *MGMT* promoter compared to 12.7 months for patients with unmethylated *MGMT* (Hegi et al., 2004, 2005).

While the currently established biomarkers hold promise in helping to improve the treatment of GBM, patients still present a poor prognosis (Taylor et al., 2019). Therefore, scientists are still working trying to find other useful biomarkers. Within the scope of this thesis, we will study the potential role of the ataxin-3 (ATXN3) protein in the context of GBM. This protein has already been shown to play a role in several other types of cancer, which will also be discussed later in this thesis.

1.5 The ATXN3 protein

ATXN3 is a protein encoded by the *ATXN3* gene with an approximate molecular weight of 42 kDa. This protein is known to be involved in Spinocerebellar ataxia type 3 (SCA3), a neurodegenerative disease caused by the unstable expansion of a cytosine-adenine-guanidine (CAG) trinucleotide within the coding region of the *ATXN3* gene.

ATXN3 is ubiquitously expressed in neuronal and peripheral tissues although with some cellular differences in the expression pattern (Trottier et al., 1998). In terms of subcellular localization, ATXN3 is predominantly found in the cytoplasm (Paulson et al., 1997), although it has been reported to be able to translocate from the cytoplasm to the nucleus and vice versa (Macedo-Ribeiro et al., 2009), and to be associated with the nuclear matrix (Tait et al., 1998). This nucleocytoplasmic shuttling is mediated by a nuclear-localization signal (NLS) and two potential nuclear export signals (NES), which are present in the *ATXN3* sequence (Antony et al., 2009; Macedo-Ribeiro et al., 2009). Furthermore, ATXN3 is an evolutionarily conserved protein, with orthologs in several organisms – mice (Do Carmo Costa et al., 2004), rat (Schmitt et al., 1997), chicken (Linhartová et al., 1999), *C. elegans* (A.J. Rodrigues et al., 2007), among others. These homologous proteins share functional domains, such as the Josephin domain (JD) and the ubiquitin-interacting motifs (UIM), nevertheless, the long polyglutamine (polyQ) tract appears to be human-specific, since it is nearly absent in other species, such as mouse and *C. elegans*, which only contain six and one glutamine, respectively (Do Carmo Costa et al., 2004; A.J. Rodrigues et al., 2007).

As a result of variations in the carboxyl terminal of the *ATXN3* gene product caused by alternative splicing and a stop codon polymorphism, several ATXN3 isoforms can be translated, differing in the number of UIMs and in their C-terminal sequence (Bettencourt et al., 2010; Goto et al., 1997; Weishäupl et al., 2019). There are two main isoforms: the original ATXN3 isoform isolated from the SCA3 human brain in 1994 contains 2 UIMs and a C-terminus of hydrophobic nature (Kawaguchi et al., 1994); later, another isoform was identified that contains 3 UIMs and a hydrophilic C-terminal region, being proposed as the most abundant isoform in the brain (Harris et al., 2010; Ichikawa et al., 2001).

ATXN3 belongs to the cysteine proteases family and, structurally, it is composed by: a structured and extremely conserved globular N-terminal JD (1-1998 aa), followed by a flexible and unstructured C-terminal that contains the polymorphic polyQ tract of variable length and two or three UIMs depending on the isoform - two UIMs before and one after the polyQ tract (**Figure 3A**) (Masino et al., 2003; Nicastro et al., 2005). The JD and UIMs are the main functional units of ATXN3 that synergistically control its activity as a deubiquitinating (DUB) enzyme, playing a role in cellular protein quality control, through Ubiquitin-proteasome system (UPS), and in regulation of the quality and stability of different substrates (B. Burnett et al., 2003; Costa et al., 2010; Neves-Carvalho et al., 2015; Winborn et al., 2008). Nuclear magnetic resonance analysis revealed that the JD is mainly composed by two subdomains – a helical hairpin and a globular catalytic subdomain comprising a catalytic site composed of a triad of cysteine (C14), histidine (H119) and asparagine (N134), characteristic of cysteine proteases (**Figure 3B**), and two binding sites for ubiquitin (Ub) (Chow et al., 2004; Nicastro et al., 2005; Scheel et al., 2003). Evidence has shown that the Q9 residue is equally important for ATXN3's catalytic activity (Mao et al., 2005; Nicastro et al., 2005). The JD has greater affinity for, and cleaves, poly-ubiquitylated proteins containing four or more Ub molecules (B. Burnett et al., 2003). The UIMs are 15-aa motifs that mediate the specific recognition and positioning of Ub chains relatively to the catalytic site for proteolytic cleavage by ATXN3 (Berke et al., 2005; Chai et al., 2004). However, evidence has shown that the UIMs may be dispensable for cleavage (Todi et al., 2009).

ATXN3 is subject to post-translational modifications, such as phosphorylation (Matos et al., 2016; Mueller et al., 2009), ubiquitylation (Todi et al., 2009, 2010) and SUMOylation (Almeida et al., 2015) (**Figure 3A**). These modifications may influence its function, subcellular localization, and interaction with other molecules (Carvalho et al., 2018; Matos et al., 2019).

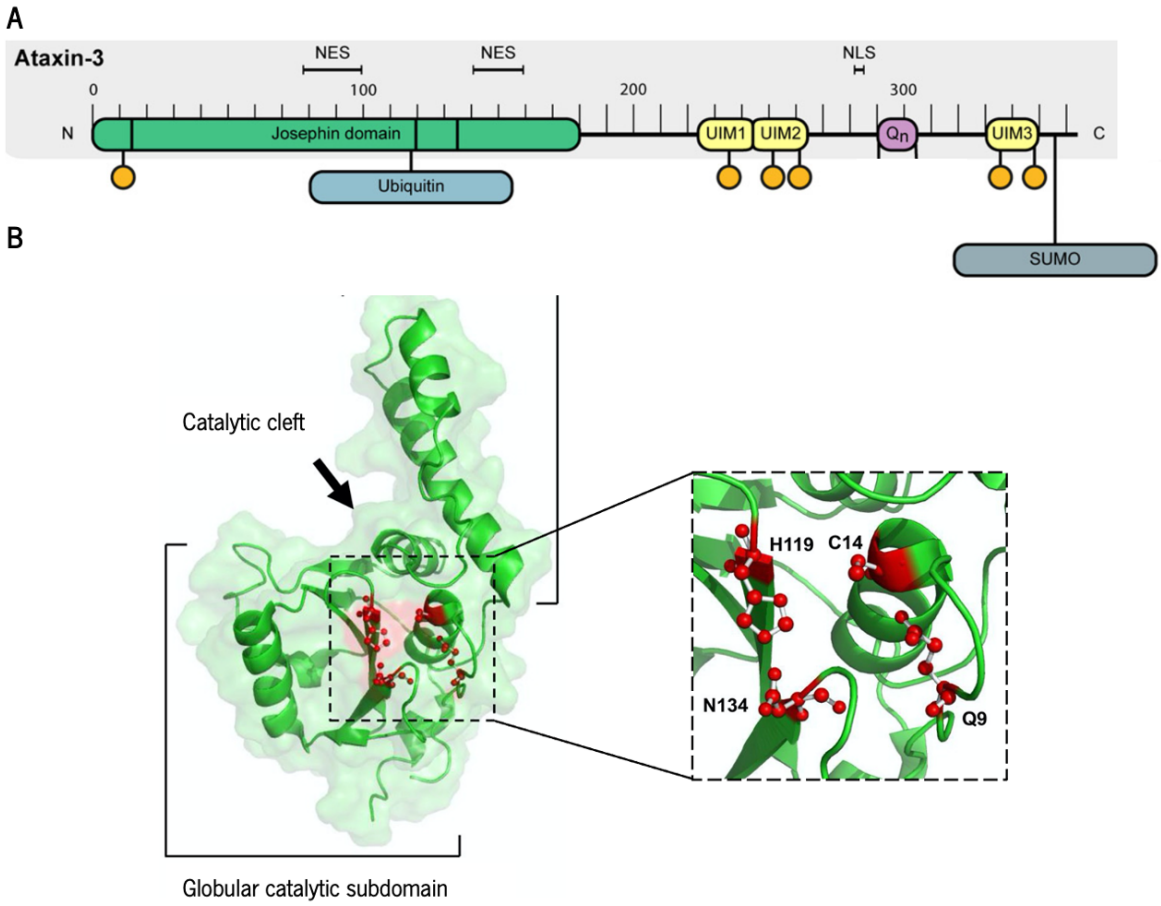

Figure 3. Schematic representation of the ATXN3 structure and domains. (A) ATXN3 is composed of a N-terminal JD with Deubiquitylating activity, followed by a C-terminal tail containing two or three UIMs that interact with ubiquitin and a polyQ sequence of variable length. Post-translational modifications targets are present. A functional NLS between the second UIM and two NES present in the JD were also described. Adapted from Matos et al., 2019. **(B)** Structure of the JD. This domain has a cleft formed by the globular catalytic and helical hairpin subdomains where the amino acids of the active site (Q9, C14, H199 and N134) are located. Adapted from Matos et al., 2011. Abbreviations: NES, nuclear export signal; NLS, nuclear localization signal; Qn, glutamine stretch of n residues; UIM, ubiquitin-interacting motif; SUMO, small ubiquitin-like modifier.

1.5.1 ATXN3 potential function(s)

Although its precise biological function(s) remain mostly unknown, it has been proposed that ATXN3 acts as a DUB, playing a role in the cellular protein quality control through the UPS. This discovery of ATXN3's deubiquitylating activity was a major step to our understanding of its function (B. Burnett et al., 2003; Winborn et al., 2008). The main function of DUB proteins consists in deubiquitylating their substrate(s), either facilitating their degradation (if at the entry of the proteasome) more easily or rescuing them from being incorrectly degraded by the proteasome (Hegde & Upadhya, 2011). As aforementioned, ATXN3 DUB activity is mediated by the JD and its binding to polyubiquitylated proteins occurs in a UIM-dependent manner (Berke et al., 2005; Mao et al., 2005). Besides that, evidence suggests that this protein is a multifunctional protein that has also been involved in other cellular pathways: (i)

Transcriptional regulation – it binds to DNA and interacts with histone deacetylases and transcriptional regulators, both repressors and activators (Evert et al., 2006; Li et al., 2002), (ii) Cytoskeleton organization – absence of ATXN3 causes disorganization in microtubules, microfilaments and intermediate filament networks (cytoskeleton components) and changes cell adhesion in many cell types (Neves-Carvalho et al., 2015; A. J. Rodrigues et al., 2010), (iii) Myogenesis – ATXN3 is crucial for the initial stages of myoblast differentiation and for regulation of integrin subunit levels (Costa et al., 2010; Neves-Carvalho et al., 2015), (iv) Aggresome formation – interaction with proteins necessary for the formation and regulation of aggresomes (B. G. Burnett & Pittman, 2005; Heir et al., 2006) and (v) Splicing regulation – absence of ATXN3 leads to a dysregulation of the pre-mRNA splicing process of several genes in neuronal cells (Neves-Carvalho et al., 2019).

1.5.2 ATXN3 in cancer

As previously stated, the discovery of ataxin-3's DUB activity was a significant step forward in our knowledge of its function. Interestingly, evidence has revealed that a huge number of DUBs play a substantial role in the development and occurrence of various types of cancer (Fraile et al., 2012; Pfoh et al., 2015), making them potential candidates for effective therapies in the treatment and prevention of this malignant disease. In fact, according to certain studies (**Table 1**), ATXN3 was also suggested to play a role in tumor cells: ATXN3 is differentially expressed in some types of cancer, being identified as a tumor suppressor gene or oncogene, depending on the cancer type.

Table 1. ATXN3 relevance in various types of cancer.

Cancer Type	Results	ATXN3 role	Reference
Familial and sporadic chronic lymphocytic leukaemia	High-length repeats at *ATXN3* associated with poor prognosis	Oncogene	Auer, R. *et al.* (2007)
Lung	ATXN3 depletion decreases cell viability	Oncogene	Sacco, JJ. *et al.* (2013)
Gastric	ATXN3 expression is decreased in gastric cancer tissue/cell lines and correlated with clinicopathological factors	Tumor suppressor gene	Zeng, L. *et al.* (2014)
Breast	Knockdown of ATXN3L inhibits breast cancer cell proliferation	Oncogene	Ge, F. *et al.* (2015)
Neuroblastoma	ATXN3 knockdown results in altered morphology, less cell adhesion and higher cell proliferation and migration	Tumor suppressor gene	Neves-Carvalho, A *et al.* (2015)
Testicular	ATXN3 is overexpressed in testicular cancer tissues, correlated with tumor stages and promotes testicular cancer cell proliferation by inhibiting PTEN	Oncogene	Shi, Z. *et al.* (2018)
Breast	High expression of ATXN3 associated with a poor prognosis of patients; ATXN3 promotes breast cancer cell migration and invasion	Oncogene	Zou, H. *et al.* (2019)
Renal cell carcinoma	*ATXN3* expression levels significantly higher in Fuhrman grade 4	Oncogene	Ergun, S. *et al.* (2020)
Oral squamous cell carcinoma	Increased *ATXN3* expression in oral squamous cell carcinoma cisplatin-resistant cell lines/tissues; ATXN3 silencing decreased migration, invasion and proliferation of cisplatin-resistant cells	Oncogene	Song, A. *et al.* (2021)

In 2007, a study described that normal *ATXN3* but with high-length repeats was associated with a poor prognosis in familial and sporadic chronic lymphocytic leukemia (Auer et al., 2007). Sacco et al. reported that ATXN3 is highly expressed in lung cancer tissues. Furthermore, the authors showed that ATXN3 depletion was sufficient to attenuate Akt phosphorylation and to promote the expression of PTEN, a classic anti-oncogene that antagonizes the PI3K/AKT/mTOR pathway, resulting in a decrease in cell viability (Sacco et al., 2014). Later, another study showed that ATXN3 expression is lower in gastric cancer than in non-cancerous gastric tissue, and that it is linked to clinicopathological factors, such as tumor size, Lauren classification, histological differentiation (negatively correlated to ATXN3 expression) and p53 protein (positively correlated to ATXN3 expression). Moreover, ATXN3L, a member of the Josephin family of DUBs, was associated with increased proliferation in breast cancer (Ge et al., 2015). In 2015, our group demonstrated that ATXN3 silencing in neuroblastoma cell line resulted in an increased cell proliferation and migration, loss of adhesion and alterations in morphology (Neves-Carvalho et al., 2015). In 2018, ATXN3 was shown to be overexpressed in testicular cancer tissues, this overexpression being associated with more advanced tumor stages and higher number of metastasis sites. Furthermore, ATXN3 overexpression was shown to promoted cell viability by inhibiting PTEN expression, suppressing p-AKT and p-mTOR levels, and activating the AKT/mTOR pathway as a result (Shi et al., 2018). ATXN3 was also reported to promote breast cancer cell migration and invasion. Furthermore, ATXN3 expression was seen to be higher in metastatic lymph nodes than in *in situ* breast carcinoma, demonstrating the potential role of ATXN3 in breast cancer metastasis. In breast cancer patients, high expression of *ATXN3* was shown to be predictive of poor prognosis (Zou et al., 2019). Using *in silico* analyses, Ergun et al. studied genes that could play a role in the pathogenesis of renal cell carcinoma. They demonstrated that *ATXN3* was expressed similarly in kidney cancer tissues and healthy kidney tissues. Furthermore, they found that *ATXN3* expression levels were not associated with TNM stages but were significantly higher at Fuhrman grade 4 (more heterogeneous in cell appearance and more aggressive in behavior) than other grades (Ergun et al., 2020). More recently, ATXN3 was also associated with oral squamous cell carcinoma (OSCC). The authors found that *ATXN3* expression was moderately increased in OSCC cell lines and tissues compared to oral epithelial keratinocytes and non-tumor tissues, respectively. Furthermore, when compared to parental cells, high levels of ATXN3 were detected in cisplatin-resistant OSCC cells. Functionally, they found that silencing ATXN3 decreased the migration, invasion and proliferation of cisplatin-resistant cells (Song et al., 2021).

Altogether, evidence strongly suggest that ATXN3 may play a role in the tumor aggressiveness and prognosis of patients with multiple types of cancer. Thus, it is important to understand its role in the

context of glioma, the most common primary malignant brain tumor type, as nothing is known about it so far.

2. | OBJECTIVES

2. OBJECTIVES

In addition to its involvement in SCA3, ATXN3 has been suggested to play an unclarified role in cancer, being expressed in several human cancer types, such as gastric (Zeng et al., 2014), testicular (Shi et al., 2018) and breast cancer (Zou et al., 2019), among others, although not fully clarified so far. Indeed, depending on the tumor type, ATXN3 performs oncogenic or tumor suppressive functions, and may be a therapeutic and prognostic candidate biomarker. Our previous data showed that ATXN3 silencing in neuroblastoma cell lines resulted in (i) alterations on cell morphology, (ii) higher cell proliferation and migration, and (iii) decreased cell adhesion, suggesting that ATXN3, in this type of cancer, plays a role as a tumor suppressor gene (Neves-Carvalho et al., 2015). However, to date, no study has explored the potential involvement of ATXN3 in brain tumors, particularly in gliomas, the most common primary malignant tumor. Thus, in this work we aimed to understand if ATXN3 has a functional role in GBM and its clinical relevance for this deadly disease. This work will be the first attempt to link ATXN3 and glioma. In this context, this project aims to (**Figure 4**):

1. Characterize ATXN3 expression levels in GBM cells and patients;
2. Evaluate the functional role of ATXN3 on cancer hallmark features *in vitro*;
3. Assess the prognostic value of *ATXN3* expression levels in GBM patients.

With this, we expect to build on the current knowledge on the biological function of ATXN3 and to determine whether it may be playing a relevant role in GBM aggressiveness.

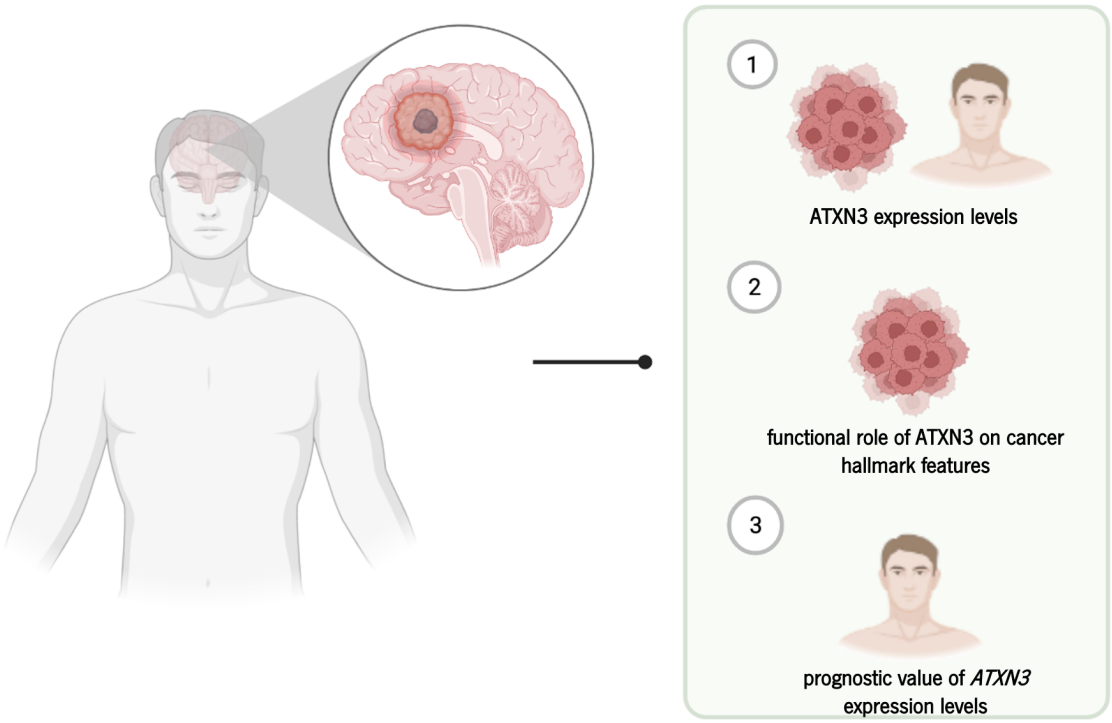

Figure 4. Schematic representation of the aims. ATXN3 expression will be characterized in GBM cells and patients and its impact on key cancer hallmarks will be evaluated, as well as on GBM patients' survival.

3. | MATERIALS AND METHODS

3. MATERIALS AND METHODS

3.1 Glioma datasets

ATXN3 gene expression and clinical data were obtained from The Cancer Genome Atlas (TCGA) (The Cancer Genome Atlas Research Network, 2008), a reference dataset in cancer research, available for download at https://portal.gdc.cancer.gov/. Microarray and RNAseq data evaluated by Agilent G4502A 244K and Illumina HiSeq 2000 Sequencing System, respectively, were collected. Microarray data include 573 GBM, 27 lower-grade gliomas (LGG; 7 grade II and 20 grade III gliomas), and 10 non-tumoral samples, while RNAseq data include 161 GBM, 466 LGG (226 grade II and 240 grade III gliomas), and 5 non-tumoral samples. When more than one portion was available per patient, the median expression value was used to avoid repeated entries from the same patient, as previously described (Gonçalves et al., 2020). Clinical data used for each patient includes information on age at diagnosis, gender, treatment received, OS, Karnofsky performance (KPS) and vital status.

To assess the expression of *ATXN3* by glioma grade the following datasets (microarray data), available for download at GlioVis website (http://gliovis.bioinfo.cnio.es/) (Bowman et al., 2017), were also used: Rembrandt (100 grade I/II, 85 grade III and 130 grade IV gliomas) (Madhavan et al., 2009), Gravendeel (32 grade I/II, 85 grade III and 159 grade IV gliomas) (Gravendeel et al., 2009), Freije (26 grade III and 59 grade IV gliomas) (Freije et al., 2004), Phillips (24 grade III and 76 grade IV gliomas) (Phillips et al., 2006), Vital (12 LGG – 3 grade I, 3 grade II and 6 grade III – and 28 grade IV gliomas) (Vital et al., 2010) and Kamoun (46 grade II, 102 grade III and 21 grade IV gliomas) (Kamoun et al., 2016) datasets. For survival analyses, only GBM patients data was used, from the following datasets: Rembrandt, Gravendeel, Freije, Phillips, Vital, Joo (Joo et al., 2013), LeeY (Y. Lee et al., 2008) and Nutt (Nutt et al., 2003) datasets. For survival analysis, the optimal cut-off determined by GlioVis (calculated using the maximum selected rank statistics) was used to define *ATXN3*-high and *ATXN3*-low glioma patients (Bowman et al., 2017). Clinical data included OS and vital status of the patients.

3.2 Cell lines and culture conditions

The commercially available human GBM cell lines U87MG and U373MG were kindly provided by Dr. Joseph Costello, University of California San Francisco. The commercially available human GBM cell lines U251MG, A172 e LN229 were purchased from American Type Culture Collection (ATCC). The commercially available human GBM cell line SNB19 was purchased from DSMZ, Germany. Immortalized human astrocytes (hTERT/E6/E7) were previously established (Tsuruga et al., 2008). The cells were cultured in Dulbecco's Modified Eagle Medium (DMEM; Sigma-Aldrich) supplemented with 10% Fetal

Bovine Serum (FBS; Sigma-Aldrich). HEK293T cells were cultured in Opti-MEM (Gibco) supplemented with 10% FBS, 1% glutaMAX (Gibco), penicillin 100 U/ml and streptomycin 100 mg/ml (Gibco). All the cells were incubated in a humidified atmosphere at 37°C and 5% (v/v) CO_2 throughout the studies. Testing for mycoplasma contamination was performed regularly. A neuroblastoma cell line (SH-SY5Y), purchased from ATCC, was used as a positive control.

3.3 Plasmid transformation into *Escherichia coli* (*E. coli)*

The bacterial transformation was performed in order to propagate the constructed plasmids. The transformation was performed into *E. coli DH5 alpha* competent cells, using the heat shock transformation method. Briefly, *E. coli* competent cells and plasmids were thawed on ice for 30 minutes and then 1 µl of the DNA was added to 50 µL of *E. coli*. The mixture was incubated on ice for 30 minutes. After incubation, the mixture was heat shocked at 42°C for 45 seconds and then placed back on ice for 30 minutes. Then, Luria Bertani (LB) medium without antibiotic was added to the cells and incubated at 37°C with shaking for 2 hours. Overnight at 37°C, 100 µL of the culture was grown on LB agar plates with the appropriate antibiotic. The next day, a colony was inoculated in LB medium with ampicillin (100 mg/mL; Sigma) at 37°C, overnight with agitation. Plasmid DNA was isolated using the GeneJET Plasmid Midiprep kit (Thermo Scientific) according to manufacturer' protocol. The concentration and purity of DNA were assessed using Nanodrop (Thermo Scientific NanoDrop 1000 Spectrophotometer).

3.4 Lentivirus production

Lentiviral particles were produced using HEK293T cells. The cells were plated in a 12-well plate at a density of 250000 cells/well in Opti-MEM supplemented with 10% FBS. On the following day, the target gene vectors (pLenti + *ATXN3* – vector containing the full-length of *ATXN3* – and the respective empty vector) and the lentiviral vectors (psPax2 and pMD2.G) were co-transfected into HEK293T cells using Fugene reagent (Promega), according to the manufacturer's recommendations. First, Fugene reagent:plasmid complex were diluted in Opti-MEM and incubated for 5 minutes at room temperature (RT), and then, cells were incubated with transfection complex during approximately 16 hours. After the incubation, the medium was renewed. Three days after transfection, the supernatant was collected and filtered through a 0.45 µm filter in order to remove cell debris.

3.5 ATXN3 overexpression in GBM cells

The A172 cell line was plated at a cell density of 40000 cells/well in a 12-well plate in DMEM supplemented with 10% FBS. On the following day, cells were infected with the lentiviral particles containing the overexpression vector (A172-ATXN3; **Figure 5**) or the respective empty vector (A172-Ctrl; Addgene, w118-1) in the presence of polybrene (8 µg/ml). Half of the total volume of virus obtained was used. The medium was changed on the next day and the cells were allowed to recover. Subsequently, successfully infected cells were selected with puromycin (0.5 µg/ml; Santa Cruz Biotecnologies) since these constructs present a puromycin resistance gene. The cell line for further experiments was generated from the polyclonal expansion of the infected/selected cells. The overexpression efficacy was confirmed by Polymerase Chain Reaction (PCR) and Western blot (WB).

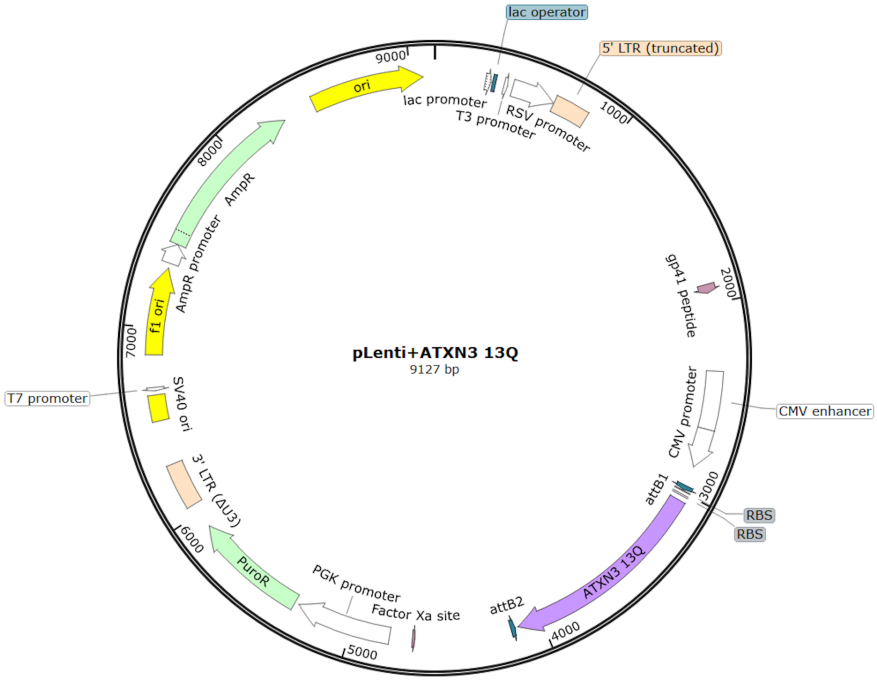

Figure 5 Constructed vector used for ATXN3 overexpression in GBM cells.

3.6 RNA extraction

Total RNA was extracted from the U251 and A172 cell lines with differential levels of *ATXN3* expression (A172-Ctrl and A172-ATXN3) using the TRIzol reagent (Invitrogen), according to the manufacturer's recommendations. Toral RNA from other human GBM cell lines, primary GBM patient-derived cultures and human immortalized astrocytes were previously obtained by the group using the same method. Briefly, TRIzol was added to the cell pellets (collected from the cell lines by centrifugation at 150 x g for 5 minutes at 4°C – Megafuge 16 Centrifuge; ThermoScientific). Each sample was homogenized and incubated to allow the cells to lyse. Then, chloroform (200 µL/mL of TRIzol) was added

to each tube and the samples were incubated and centrifuged at 21100 x g (Fresco 21 Microcentrifuge; ThermoScientific) for 15 minutes at 4°C to promote phase separation. The upper clear aqueous phase (containing the RNA) was carefully collected, and isopropanol (500 µL/mL of TRIzol) was added to precipitate the RNA. After incubation the samples were centrifuged at 12000 x g for 10 minutes at 4°C. The supernatant was removed and finally, the precipitated RNA was washed in 75% ethanol (1mL/mL of TRIzol) and centrifuged at 7500 x g for 5 minutes at 4°C. The supernatant was discarded, and the RNA was diluted in RNase and DNase free water. The quantity and purity of RNA were assessed using Nanodrop (Thermo Scientific NanoDrop 1000 Spectrophotometer). RNA integrity was confirmed by running a 1% agarose gel prepared in 1x Tris-acetate-EDTA (TAE) buffer.

3.7 DNA extraction

To determine the CAG repeat of the *ATXN3* gene in the glioma cell lines, DNA from the A172 cell line and U87MG was extracted using the Citogene DNA Isolation Kit (Citomed), according to the manufacturer's recommendations. Briefly, Cell Lysis solution was added to the cells in order to break the cell membranes and release the DNA and protein. After centrifugation at 15700 x g (Centrifuge 5415D; Eppendorf) for 6 minutes, a compact protein pellet is formed and the DNA (present in the supernatant) is precipitated with 100% isopropanol. The samples were centrifuged at 15700 x g for 4 minutes and, afterwards, the DNA, in the form of a white pellet, was washed with 70% ethanol. A new centrifugation at 15700 x g for 4 minutes was performed and finally, DNA hydration solution was added to the pellet. The quantity and purity of DNA were assessed using Nanodrop (Thermo Scientific NanoDrop 1000 Spectrophotometer).

3.8 cDNA synthesis

After RNA quantification, a treatment with DNase was performed to remove possible genomic DNA, using the DNase I, RNase-free kit (Thermo Scientific), according to the manufacturer's recommendations. The reaction was prepared with 1 µg of RNA, Reaction Buffer with $MgCl_2$ (1x), DNase I (0.1 U/µL) and water to a volume of 10 µL. The reaction took place in the thermo cycler (Bio-Rad T100 Thermal Cycler) at 37°C for 30 minutes. The reaction was terminated with the addition of 1 µL of EDTA (5 mM) per sample and incubation at 65°C for 10 minutes. Then, the cDNA was synthesized from 1 µg of RNA using the iScript cDNA Synthesis Kit (Biorad). Briefly, a reaction mixture was prepared adding nuclease-free water, 1x iScript Reaction Mix (contains dNTP's, primers) and iScript Reverse Transcriptase. The sample was placed in the thermo cycler (Bio-Rad T100 Thermal Cycler) and programmed with the following

protocol: 25°C for 5 minutes (primer binding), 46°C for 20 minutes (reverse transcription), 95°C for 1 minute (enzyme inactivation) and 4°C infinitely.

3.9 Quantitative Polymerase Chain Reaction (qPCR)

The levels of *ATXN3* and *HPRT1*, used as a reference gene, were assessed by qPCR using the SoFast Eva Green RT-PCR reagent kit (Bio-Rad), according to the manufacturer's recommendations. A reaction mix was prepared by adding DNase and RNase free water, the EvaGreen enzyme, the forward and reverse primers (0.2 µM *HPRT1* and 0.5 µM *ATXN3*; **Table 2**) and the cDNA samples, obtained as described above. The samples were placed in the 7500 Fast Real-Time PCR System (Applied Biosystems) and the qRT-PCR cycling conditions used were: 95°C for 30 seconds (enzyme activation), 95°C for 5 seconds (DNA denaturation) and 60°C for 30 seconds (primers annealing/extension). The last 2 steps were repeated 40 times, and after that a melting curve was performed to assess whether the reaction produced unique and specific products. In each run, negative controls (mix solution, but without any cDNA) were included to screen for possible contamination. The expression levels were normalized to the relative expression of the *HPRT1* gene. Results were presented using the ΔΔct method (Livak & Schmittgen, 2001). The variation between the Cq of samples was calculated and the relative expression was determined.

3.10 PCR

A PCR was performed to evaluate the *ATXN3* expression in the A172-overexpression cell line, using the AmpliTaq Gold 360 DNA Polymerase kit (Applied Biosysystems), according to the manufacturer's recommendations. A reaction mix was prepared by adding DNase and RNase free water, AmpliTaq Gold 360 Buffer (1x), Magnesium Chloride (1.5 mM), dNTP mix (200 µM each), AmpliTaq Gold 360 DNA Polymerase (2 U), the forward and reverse primers (0.8 µM; **Table 2** and the cDNA sample. The following protocol was used in the thermo cycler (Bio-Rad T100 Thermal Cycler): 95°C for 10 minutes (DNA initial denaturation), 95°C for 30 seconds (DNA denaturation), 60°C for 30 seconds (primers annealing), 72°C for 60 seconds (primers extension) and 72°C for 7 minutes (final extension). The 3 intermediate steps were repeated 35 times. Thereafter, the PCR products were run on a 2% agarose gel prepared in 1x Tris-borate-EDTA (TBE) buffer.

The determination of CAG repeat length was performed in the U87MG and A172 glioma cell lines by PCR amplification, using the previously extracted DNA. For this, a reaction mixture was prepared by adding nuclease-free water, MyTaq Reaction Buffer (1x), MyTaq HS DNA polymerase (Bioline) and primers

(0.5 µM; **Table 2**). The following protocol was used in the thermo cycler (Bio-Rad T100 Thermal Cycler): 95°C for 3 minutes (denaturation), 95°C for 15 seconds (annealing), 55°C for 15 seconds (extension), 72°C for 15 seconds (final extension). The last 3 steps were repeated 30 times. The PCR products were analyzed by fragment analysis in comparison to a size standard, as described in (Silva-Fernandes et al., 2014).

Table 2. Sequence of primers used in the qRT-PCR, PCR, and in the determination of CAG length.

	Primers	Sequence (5'-3')
qPCR	*ATXN3* Forward	GGAACAATGCGTCGGTTG
	ATXN3 Reverse	GCCCTAACTTTAGACATGTTAC
	HPRT1 Forward	TGAGGATTTGGAAAGGGTGT
	HPRT1 Reverse	GAGCACACAGAGGCCTACAA
PCR	*ATXN3* Forward	CCGGGGATCCATGGAGTCCATCTTCCACGA
	ATXN3 Reverse	CCGGCTCGAGTTTTTTTCCTTCTGTTTTCA
CAG repeat	*ATXN3* Forward	GGCTGGCCTTTCACATGGAT
	ATXN3 Reverse	CGGAAGAGACGAGAAGCCTAC (with 5' 6-FAM modification)

3.11 Western Blot (WB)

Cells were washed using PBS 1x and removed by scratch in the lysis buffer [RIPA buffer: 50 mM Tris-HCl pH 7.4, 250 mM NaCl, 2 mM EDTA, 10% Glycerol and inhibitors of proteases 1x (Roche)]. The cell lysate was incubated for 15 min and then centrifuged at 21100 x g (Fresco 21 Microcentrifuge; ThermoScientific) for 15 min at 4°C. Using the obtained supernatant, the total protein concentration was determined by the Bradford method, using the kit Protein Assay Dye Reagent Concentrate (Bio-Rad). Protein extracts were denatured and reduced with 2x Laemmli Sample Buffer (Bio-Rad), to which 20 mM dithiothreitol (DTT) was added. Then the protein (10-20 µg) was separated in a 10% SDS-polyacrylamide resolving gel and a 4% stacking gel by electrophoresis. A molecular weight marker (GRS protein marker multicolour - GRISP) was added. The gel was transferred to nitrocellulose membranes using the Trans-Blot Turbo Transfer System (Bio-Rad), and the Ponceau S dye was used to confirm the efficiency of the transfer. Before immunodetection, the membranes were blocked with 5% milk for 1 hour at RT, in order to prevent non-specific binding of the antibody. Subsequently, antibodies against ATXN3 (1H9; Ref. MAB5360; Millipore), GAPDH (Ref: ab9485; Abcam) and b-actin (Ref. 8227; Abcam) were used for immunodetection, in which the membranes were incubated overnight at 4°C. After incubation with the primary antibody, the membranes were washed with washing buffer (2.5% milk diluted in 1x TBS and

0.1% Tween) for 10 min. Then, the membranes were incubated for 1 hour at RT with peroxidase-conjugated secondary anti-mouse (Ref. 1706516; Bio-Rad) or anti-rabbit IgG antibodies (Ref. 1706515; Bio-Rad). Blots were revealed using an enhanced chemiluminescence (ECL) solution (Clarity Western ECL Substrate; Bio-rad). Chemiluminescence was measured using the Sapphire Biomolecular Imager (Azure Biosystems) and with Wide Dynamic Range of exposure. Band quantification was performed using AzureSpot, according to the manufacturer's instructions. Protein expression was normalized using b-actin (GBM parental cells) or GAPDH (A172-overexpression model) as a control protein.

3.12 Cell viability assays

3.12.1 Trypan Blue assay

A172 (A172-Ctrl and A172-ATXN3) cells were plated, in triplicate, in 6-well plates at an initial density of 15000 cells/well and allowed to adhere and grow for 4 and 6 days. At day 4 and 6, the cells were recovered by trypsinization and mixed with trypan blue dye (1:1 ratio; Gibco). Viable cells possess intact cell membranes that exclude the dye, unlike dead cells, that have compromised membrane integrity. The number of viable cells from each well was counted with the help of Neubauer chamber, under the microscope in duplicates. The total number of cells was calculated using the formula:

$$mean\ of\ viable\ cells\ \times\ dilution\ factor\ \times\ 10^4 \times total\ volume.$$

3.12.2 MTS assay

A172 (A172-Ctrl and A172-ATXN3) cells were plated, in triplicate, in 24-well plates at an initial density of 2000 cells/well and allowed to adhere and grow for 6 days. At day 6, the cells were incubated with 10% of the MTS solution (CellTiter 96® AQueous One Solution Cell Proliferation Assay; Promega) in DMEM supplemented with 10% FBS, in the dark, in a humidified atmosphere, at 37°C and 5% CO_2 for approximately 2 hours. MTS (3-(4,5-Dimethylthiazol-2-yl)-5-(3-carboxymethoxyphenyl)-2-(4-sulfophenyl)-2H-tetrazolium) is reduced to a purple soluble formazan product in metabolically viable cells by a NAD(P)H-dependent mitochondrial dehydrogenase enzyme, thus providing information about the metabolic viability of the cells. After incubation, the formazan dye produced by viable cells was quantified by measuring the absorbance at 490 nm.

3.13 Cell proliferation assay

Cell proliferation was assessed based on the measurement of bromodeoxyuridine (BrdU), a synthetic analogue of thymidine incorporated during DNA synthesis, using the Cell Proliferation ELISA, BrdU colorimetric assay kit (Roche), and according to the manufacturer's recommendations. The A172

(A172-Ctrl and A172-ATXN3) cells were plated, in triplicate, in 96-well plates, at an initial density of 2000 cells/well and incubated for 4 days. Subsequently, BrdU was added to the cell culture, and they were re-incubated for 8 hours. Then, an enzyme-linked immunosorbent assay (ELISA) was performed. FixDenat was added to the cells, a solution that fixes the cells and denatures the DNA to enable antibody binding. After 30 minutes of incubation at RT, anti-BrdU-POD antibody was added to the cells and incubated for another 90 minutes at RT. Subsequently, the antibody conjugate was removed, and the wells were washed 3 times with Washing Solution to allow for removal of unbound antibodies. Finally, Substrate Solution was added to allow photometric detection at 370 nm.

3.14 Cell migration assay

Cell migration capacity was assessed using the wound healing assay. The A172 (A172-Ctrl and A172-ATXN3) cells were plated, in triplicates, at an initial cell density of 70000 cells in each side of Ibidi 2-well inserts (Ibidi) and left to adhere overnight. Subsequently, the inserts were removed (0 hours timepoint), leaving a 500 µm cell-free gap. The created artificial wound from each well was photographed over time in the same position using the CKX41 inverted microscope (Olympus), until the wound was completely closed (approximately 24 hours). The relative cell migration (gap size) was measured using an automated software (beWound - Cell Migration Tool, v1.7, ICVS, Portugal), and the gap size was verified and corrected manually, when necessary. Ten positions equally spaced and perpendicular to the wound were measured. The percentage of wound closure was calculated by measuring the width of the wound relatively to the initial width of the wound (time 0 h).

3.15 Cell invasion assay

Cell invasion was assessed using the Boyden chamber assay. BD BioCoat™ Matrigel™ Invasion Chambers (Corning®) were used, according to the manufacturer's recommendations. The A172 (A172-Ctrl and A172-ATXN3) cells were plated in the upper compartment of the chamber at an initial density of 20000 cells/well in DMEM supplemented with 1% of FBS. Epidermal growth factor (EGF; 20 µM; Invitrogen), a chemotactic agent, was added to the lower compartment containing DMEM supplemented with 10% FBS. The cells were left to incubate for 22 hours, and, after this period, non-invading cells at the top of the chamber were gently removed by a cotton swab and the invading cells, attached to the membrane, were fixed with 100% cold methanol and stained using DAPI with mounting medium (Vectashield; Vector Laboratories). Whole membranes were scanned using an Olympus Widefield Inverted

IX81 microscope (Olympus; objective lens magnification: 4x) and the total number of invading cells was counted using the ImageJ software (version 1.53).

3.16 Cell cycle assay

The cell cycle was assessed by flow cytometry using Propidium Iodide (PI) staining. The A172 (A172-Ctrl and A172-ATXN3) cells were plated at an initial density of 200000 cells per T25 flask in DMEM supplemented with 10% FBS. Two days later, cells were trypsinized, washed with 1x PBS and fixed in 70% cold ethanol. Afterwards, the cells were centrifuged at 266 x g (Megafuge 16 Centrifuge; ThermoScientific) for 5 minutes at 4°C and were again washed with 1x PBS. Then, fixed cells were incubated with PI staining solution [0.1% triton-X-100, 20 µg/mL PI (ThermoFisher Scientific) and 250 µg/mL RNase (Invitrogen) in PBS] in the dark for 1 hour at 50°C. Flow cytometry was used for cell cycle analysis of PI-stained cells. At least 10000 single cells events per sample were acquired in a BD LSRII flow cytometer (BD Biosciences) using the FACS DIVA software (BD Biosciences). The collected data was analyzed using the FlowJo software (v10.8.0; Tree Star). The number of cells in each phase of the cell cycle was quantified using the Dean-Jett-Fox model.

3.17 Cell death assay

Cell death was assessed by flow cytometry using annexin V/PI staining. The A172 (A172-Ctrl and A172-ATXN3) cells were plated at an initial density of 40000 cells per T25 flask. After 24 hours, cells were treated with TMZ (800 µM) or with DMSO (dimethylsulfoxide), used as vehicle. The treatment was renewed 2 days later. Cell death was assessed after 6 days of treatment with TMZ and DMSO. Cells were stained with Annexin V-FITC (BD Bioscience) and PI (5 µg/mL; ThermoFisher Scientific), followed by flow cytometric analyses. At least 10000 single cells events per sample were acquired in a BD LSRII flow cytometer (BD Biosciences) using the FACS DIVA software (BD Biosciences). Results were analyzed using FlowJo software (v10.8.0; Tree Star).

3.18 Statistical analyses

ATXN3 expression in gliomas of different grade was evaluated using the two-sided unpaired *t*-test or one-way ANOVA. When normality was not verified by the Shapiro-Wilk test, the non-parametric Mann-Whitney and Krustal-Wallis tests were used. For the wound healing, cell death and cell cycle assays a two-way ANOVA followed by the post-hoc Sidak's test for multiple comparison testing was used. For the others assays, homoscedasticity was verified with Levene's test and differences between groups were assessed

by a two-sided unpaired *t*-test, with Welch's correction applied accordingly. The prognostic value of *ATNX3* expression was assessed by univariate (presented on a Kaplan-Meier curve) and multivariate analyses using, respectively, the log-rank test or the Cox regression model, corrected to putative confounding factors (patient's age, gender and KPS) in order to test the independence of the results obtained. These analyses were made with SPSS 19.0 software (SPSS, Inc.). The Comprehensive Meta Analysis (CMA) v3 software (Biostat, Inc.) was used to conduct a meta-analysis that included all datasets. Hazard ratios (HR) and 95% confidence intervals (CI) were determined by univariate and multivariate (for TCGA) Cox analysis. Graphical representation was performed using the GraphPad Prism 8.4.3 software. Results are presented as mean ± SD, and for all statistical tests significance was considered when $p < 0.05$, for a 95% CI.

4. | RESULTS

4. RESULTS

4.1 *ATXN3* expression decreases with glioma grade

Despite the fact that ATXN3 expression has been evaluated in different human cancers, little is known about the precise role of ATXN3 in these tumors, and nothing has been described about its role in brain tumors, particularly in gliomas. With this in mind, we first analyzed *ATXN3* expression levels in normal and patients with glioma grade II, III and IV (GBM) samples deposited in the TCGA database, using RNA sequencing (161 GBM, 466 LGG and 5 non-tumoral samples) and microarray data (573 GBM, 27 LGG and 10 non-tumoral samples), in order to evaluate how *ATXN3* is expressed and distributed among glioma grades. *ATXN3* expression was found to significantly decrease with glioma grade, and therefore with its malignancy, being less expressed in GBM patients (the most malignant glioma) when compared with normal controls and with patients with glioma grades II and III (**Figure 6A and B,** left panel). We observed the same result both in the RNAseq and microarray data, although in the latter statistically significance was only observed between normal controls and GBM patients.

The IDH mutation and the 1p/19 codeletion status, two extremely important diagnostic molecular markers, were introduced in the 2016 WHO classification of CNS tumors, allowing for a more refined classification of gliomas (Louis et al., 2016). Thus, using the TCGA data, we analyzed whether *ATXN3* expression is associated with the IDH mutation and/or the 1p/19q codeletion status. RNAseq data analysis showed that in the subset of patients with glioma grade II there were no significant differences between the stratified patients. Within patients with glioma grade III, we found that IDH-mutant and 1p/19q codeletion patients had the highest levels of *ATXN3* expression and IDH-wildtype patients had the lowest levels of *ATXN3* expression. Accordingly, IDH-wildtype GBMs presented significantly lower levels of *ATXN3* when compared to IDH-mutant GBMs (**Figure 6A**, right panel). The same was observed when the analyses were performed using microarray data (**Figure 6B,** right panel). Here, LGG patients were not stratified according to the 2016 CNS classification due to the limited amount of available TCGA microarray data. These results suggest that *ATXN3* expression is associated with IDH mutation and 1p/19q codeletion, and therefore with a better outcome.

In addition, 6 additional datasets were analyzed: Rembrandt (n = 315; **Figure 7A**), Gravendeel (n = 276; **Figure 7B**), Freije (n = 85; **Figure 7C**), Phillips (n = 100; **Figure 7D**), Vital (n = 40; **Figure 7E**) and Kamoun (n = 169; **Figure 7F**). With these multiple analyses we greatly increased our confidence that *ATXN3* expression significantly decreases with increasing glioma grade. The exception was observed using the Kamoun, Phillips and Vital datasets, where this difference was not verified, although in the Phillips and Vital datasets the same trend is observed.

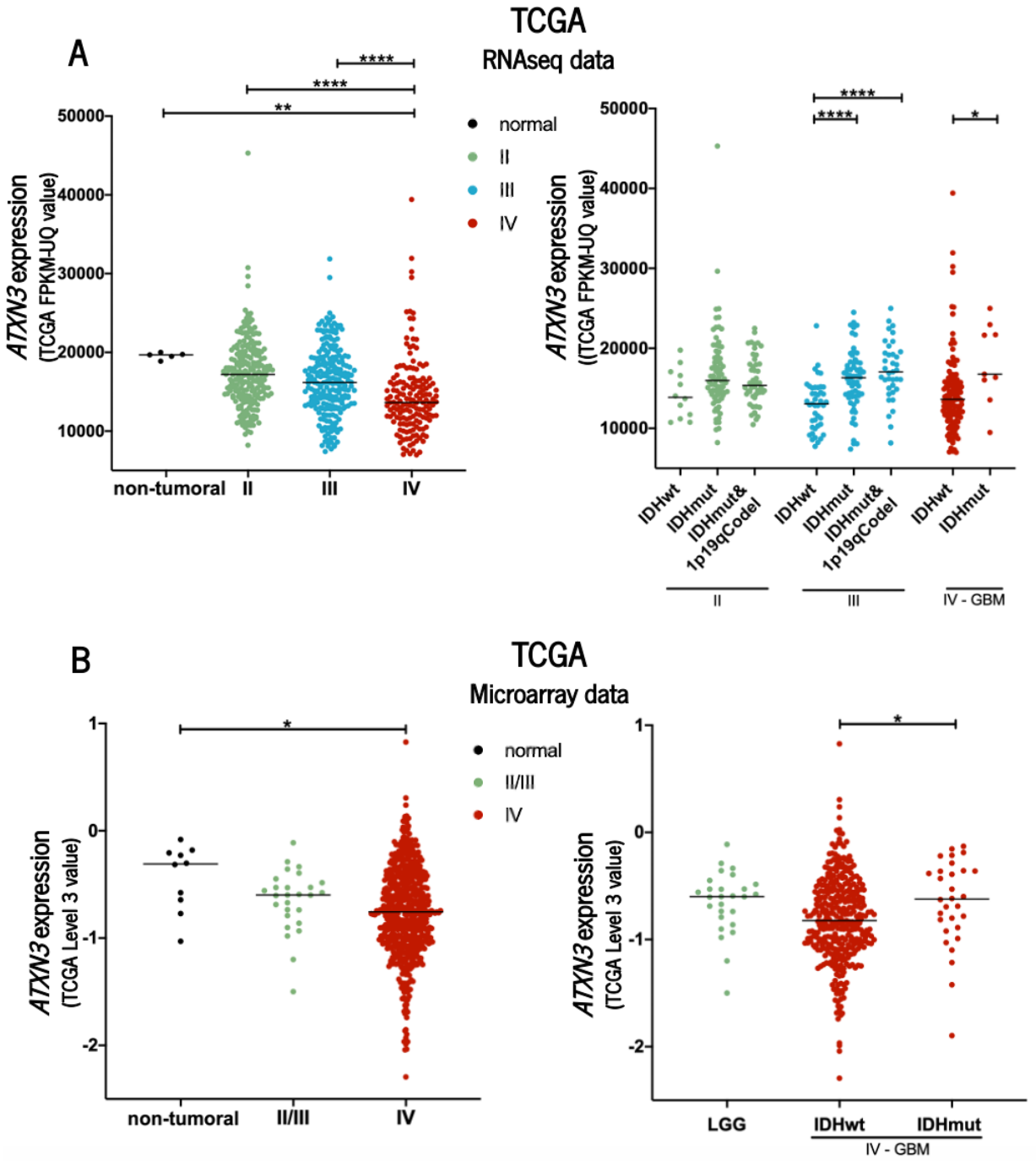

Figure 6. ATXN3 expression decreases with glioma grade and is associated with IDH mutation and 1p/19q codeletion in TCGA. (A) RNAseq expression levels of ATXN3 in unmatched normal *samples* (5 samples), in grade II gliomas *samples* (226 patients; 12 IDHwt, 75 IDHmut non-codeleted, and 48 IDHmut 1p/19q codeleted), in grade III gliomas *samples* (244 patients; 43 IDHwt, 62 IDHmut non-codeleted and 37 IDHmut 1p/19q codeleted), and in GBM *samples* (161 patients; 141 IDHwt and 9 IDHmut) from the TCGA. **(B)** Microarray expression levels of ATXN3 in unmatched normal *samples* (10 samples), in LGG *samples* (27 patients; 7 grade II and 20 grade III gliomas) and GBM *samples* (573 patients; 368 IDHwt and 30 IDHmut) from TCGA. *, $p < 0.05$; **, $p < 0.01$; and ****,$p < 0.0001$. (Unpaired t-test/Mann-Whitney to compare subtypes in the same glioma grade and One-way ANOVA/Kruskal-Wallis to compare glioma grades). IDHwt: IDH-wildtype; IDHmut: IDH-mutant; 1p/19qCodel: 1p/19q Codeletion.) from TCGA.

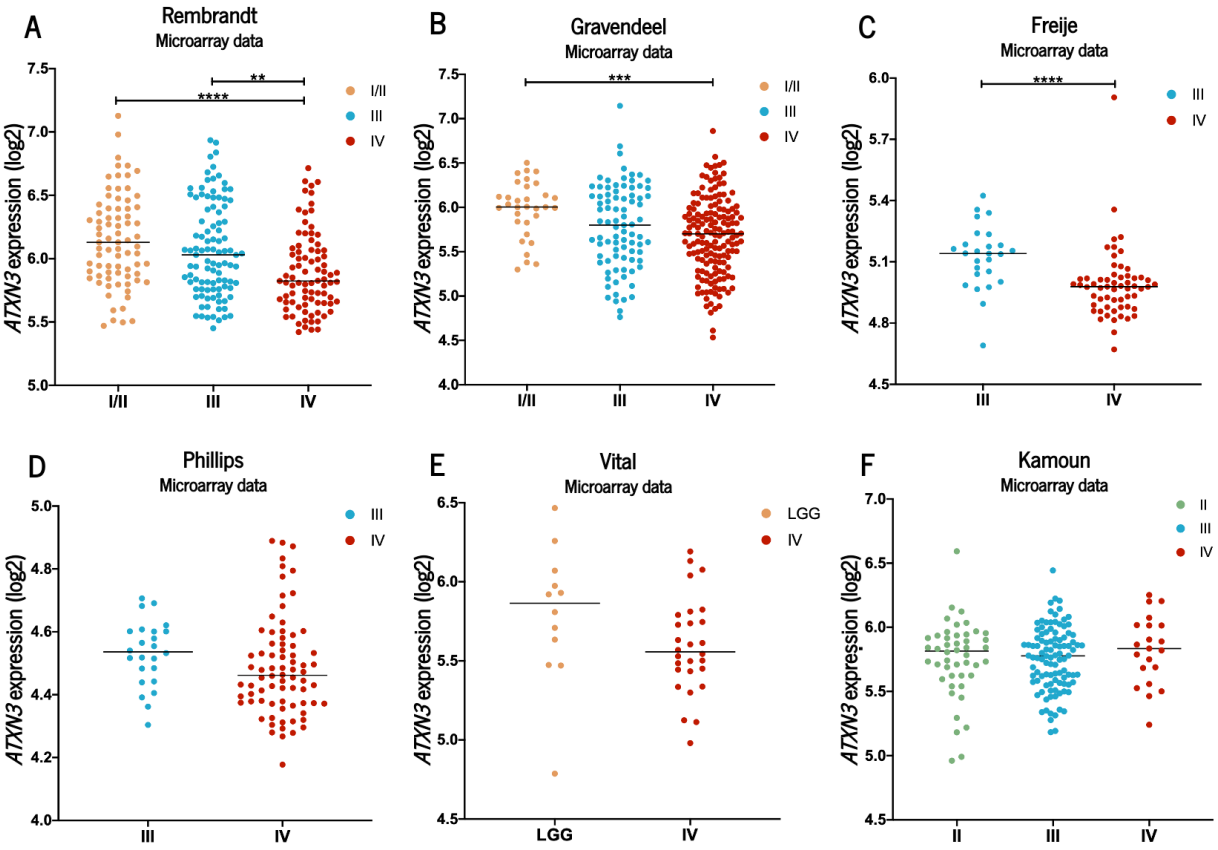

Figure 7. ATXN3 expression decreases with glioma grade in several glioma cohorts. (A-F) Microarray expression levels of ATXN3 evaluated in the (A) Rembrandt (100 grade I/II, 85 grade III, and 130 grade IV gliomas), (B) Gravendeel (32 grade I/II, 85 grade III, and 159 grade IV gliomas), (C) Freije (26 grade III and 59 grade IV gliomas), (D) Phillips (24 grade III and 76 grade IV gliomas), (E) Vital (12 LGG - 3 grade I, 3 grade II and 6 grade III - and 28 grade IV gliomas) and (F) Kamoun (46 grade II, 102 grade III, and 21 grade IV gliomas) datasets. **, $p < 0.01$; ***, $p < 0.005$; and ****, $p < 0.0001$. (Unpaired t-test/Mann-Whitney to compare 2 groups and One-way ANOVA/Kruskal-Wallis to compare 3 groups). IDHwt: IDH-wildtype; IDHmut: IDH-mutant; 1p/19qCodel: 1p/19q Codeletion.

Together, these results strongly suggest that high levels of *ATXN3* expression are associated with lower grades of glioma. Furthermore, *ATXN3* expression seems to be associated with the IDH mutation and 1p/19q codeletion in gliomas.

4.2 ATXN3 is differentially expressed in GBM cell lines

Following our evaluation of *ATXN3* expression in various glioma grades (**Figure 6 and Figure 7**), we wanted to know more about ATXN3 expression in GBM, the most aggressive subtype of glioma. To do so, we first characterized ATXN3 expression in a panel of GBM cell models. We were able to detect ATXN3 expression both at the mRNA (**Figure 8A**) and protein levels (**Figure 8B**) in all cell models. We could also see that the A172 cell line had the lowest levels of ATXN3 expression, both at the mRNA and protein level, while the highest levels were observed in the U373MG, U87MG and GL45 cells at the mRNA level and in U373MG cells at the protein level.

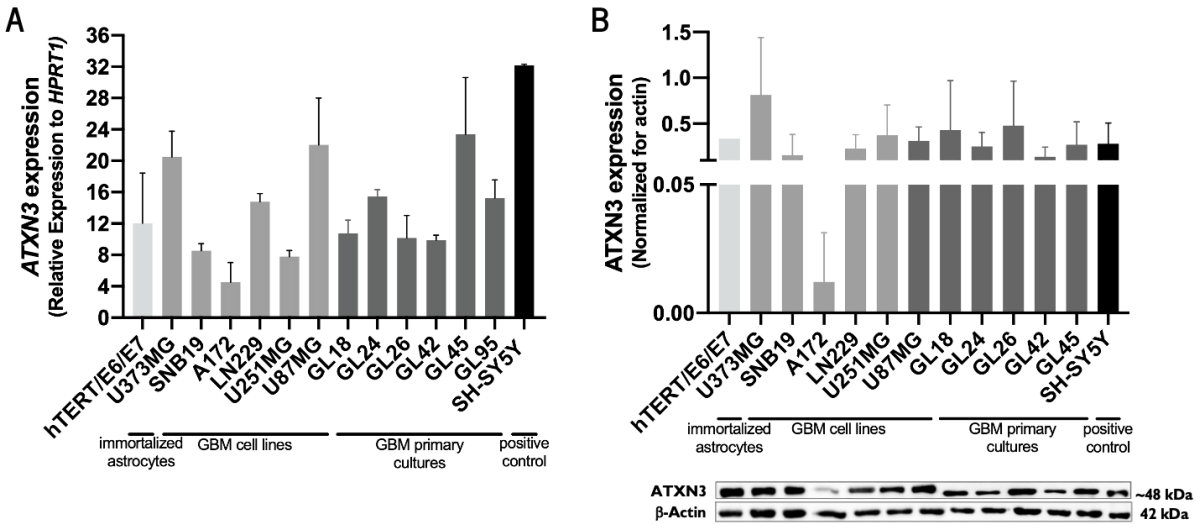

Figure 8. ATXN3 is differentially expressed in GBM cells. (A-B) ATXN3 expression levels were characterized in commercial GBM cell lines (U373MG, SNB19, A172, LN229, U251MG and U87MG), in primary cultures established by our group (GL18, GL24, GL26, GL42, GL45 and GL95), in immortalized astrocytes and in a neuroblastoma cell line used as a positive control (SH-SY5Y), by qRT-PCR (A) and WB (B). (A) ATXN3 expression levels at the mRNA level (normalized to HPRT1). (B) Top: ATXN3 expression levels at the protein level (normalized to b-actin). Bottom: Representative image of the WB (3 independent assays were performed; 1 assay of hTERT/E6/E7 in WB).

Together, these results show that ATXN3 is differentially expressed in GBM cells.

4.3 ATXN3 decreases GBM aggressiveness, having a role as a tumor suppressor gene

We further explored the impact of ATXN3 expression levels on cancer hallmarks *in vitro*. We started by establishing a cell line with stable wild-type ATXN3 overexpression. For this, we chose the A172 cell line (the GBM cell line that presented the lowest levels of ATXN3 expression among the panel of cells evaluated) to be transduced with lentiviral particles carrying an overexpression vector containing the *ATXN3* coding region (A172-ATXN3) or the respective empty vector (A172-Ctrl), as control. The efficiency of the infection was validated by WB and PCR. As observed, the A172-ATXN3 cell line has higher levels of ATXN3 expression when compared to the control line (**Figure 9A**).

Once ATXN3 overexpression in the A172 GBM cell line was established, the functional impact of ATXN3 in these cells was evaluated. The trypan blue exclusion assay and the MTS assay were used to determine cell viability. Throughout time, the cell line with ATXN3 overexpression showed significantly lower viability than the control cell line (p = 0.5957 at day 4, and p = 0.02 at day 6; **Figure 9B**). In agreement, in the MTS assay, ATXN3 overexpression significantly decreased the metabolic cell viability of the GBM cells (p = 0.0115; **Figure 9C**). Posteriorly, we evaluated the impact of ATXN3 on cell proliferation through the BrdU assay. We found that ATXN3 overexpression did not affect the proliferation capacity of the cells (p = 0.2421; **Figure 9D**). In addition to the BrdU proliferation assay, we evaluated

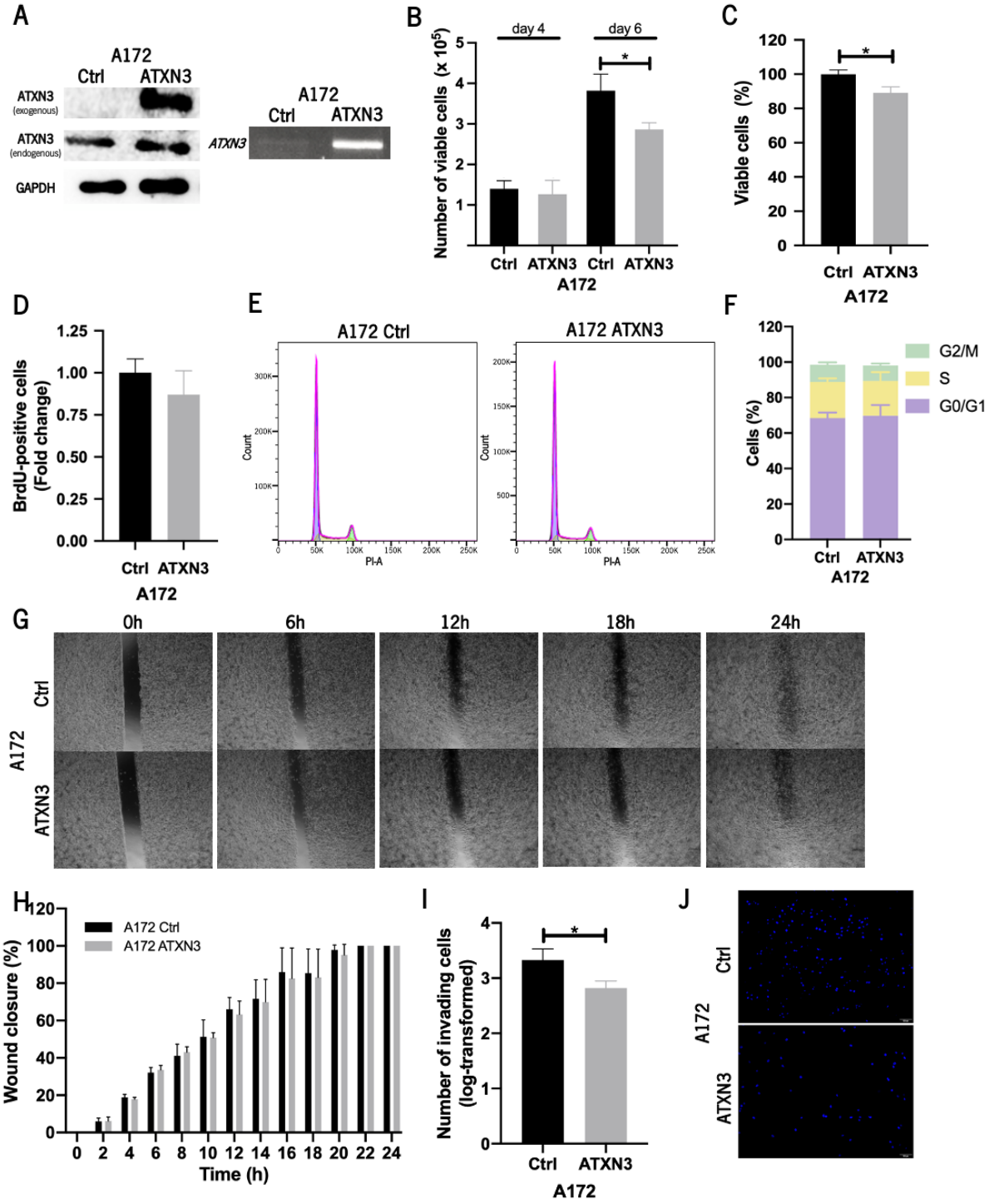

Figure 9. ATXN3 expression decreases GBM aggressiveness. (A) ATXN3 overexpression in the A172 cell line was confirmed by WB (left) and PCR (right). **(B)** Cell viability of A172-ATXN3 and A172-Ctrl cell lines was evaluated by Trypan Blue assay (n=3). **(C)** Cell viability of A172-ATXN3 and A172-Ctrl cell lines was evaluated by MTS assay (n=3). **(D)** Cell proliferation of A172-ATXN3 and A172-Ctrl cell lines was assessed by the BrdU assay (n=3). **(E-F)** Cell cycle analysis was performed by flow cytometry after PI staining. (E) Representative image of cell cycle results. The initial peak and the last peak represent the G0/G1 and G2/M phases, respectively, while between the peaks is the S phase. (F) Quantification of the percentage of cells in each phase of the cycle using an algorithm (Dean-Jett-Fox model; FlowJo software). **(G-H)** The migration capacity of the

(*continued on next page*)

(*cont.)*

A172-ATXN3 and A172-Ctrl cell lines were evaluated by the wound healing migration assay (0 h-12 h n = 3, and 12 h-24 h n = 4). (G) Quantification of the percentage of wound closure over time. (H) Representative images (4x magnification; scale bar = 20000 µm) **(I-J)** Invasion capacity of the A172-ATXN3 and A172-Ctrl cell lines was evaluated by the Matrigel Chamber invasion assay (n=3). (I) Quantification of the number of invasive cells. (J) Representative imagens with cell nuclei stained with DAPI (scale bar = 100 µm). *, $p < 0.05$ (Unpaired *t*-test and two-way ANOVA with post-hoc Sidak's test for the wound healing and cell cycle assays).

the effect of ATXN3 on GBM cell cycling. Flow cytometry was used to quantify the proportion of cells in each stage of the cell cycle stained with PI, a DNA binding dye. There were no statistically significant differences comparing cells with ATXN3 overexpression and control cells, in what regards the percentage of cells in each cell cycle phase ($p = 0.9646$ for G0/G1, $p = 0.9919$ S, $p = 0.9857$ G2/M; **Figure 9E and F**). This result suggests that ATXN3 does not affect cell cycle progression of GBM cells. In order to assess whether ATXN3 modulates the ability of A172 cells to migrate, we performed a wound healing assay for 24 hours. We did not observe statistically significant differences between control and ATXN3 overexpressing cell lines, concluding that ATXN3 appears to not affect the migration capacity of the cells (**Figure 9G and H**). Furthermore, as GBMs have a great capacity to invade brain tissue (Brandes et al., 2008; C. Smith & Ironside, 2007), we tested whether ATXN3 mediates GBM invasion, through the Boyden Chamber assay. Interestingly, we observed that ATXN3 overexpression significantly decreased the invasiveness of cells ($p = 0.0217$; **Figure 9I and J**).

Overall, although ATXN3 has no impact on the proliferation, cell cycle or migration capacity of the GBM cells, ATXN3 expression present a functional impact on GBM cells, by affecting their viability and capacity to invade, which suggests that it may acts as a tumor suppressor molecule, reducing GBM aggressiveness *in vitro*.

4.4 ATXN3 does not affect the sensitivity of GBM cells to TMZ

Although TMZ is the first-line chemotherapeutic agent used for GBM patients, many patients develop resistance to the drug, leading to treatment failure (S. Y. Lee, 2016). In this context, we tested whether ATXN3 expression may affect GBM cell sensitivity/resistance to TMZ. Treatment with TMZ or DMSO (used as vehicle) was applied for 6 days, and cell death was assessed by flow cytometry using Annexin V and PI staining. Treatment of both cells (A172-Ctrl and A172-ATXN3) with TMZ led to a significant decrease in the percentage of viable cells ($p = 0.0078$ for A172-Ctrl and $p = 0.0008$ for A172-ATXN3), as well as a significant increase in Annexin V + PI positive cells ($p = 0.0244$ A172-Ctrl and $p = 0.0027$ A172-ATXN3) and in Annexin V positive cells ($p = 0.0307$ A172-Ctrl and $p = 0.0268$ A172-ATXN3), compared to treatment with vehicle. However, ATXN3 overexpression did not affect the sensitivity

of the GBM cells to TMZ-mediated treatment (**Figure 10**), since the number of viable cells (p = 0.9516) and the number of apoptotic cells (p = 0.9050) is similar in ATXN3 overexpressing cells and in control cells.

These results suggest that ATXN3 does not affect the sensitivity to TMZ treatment in this GBM cellular model.

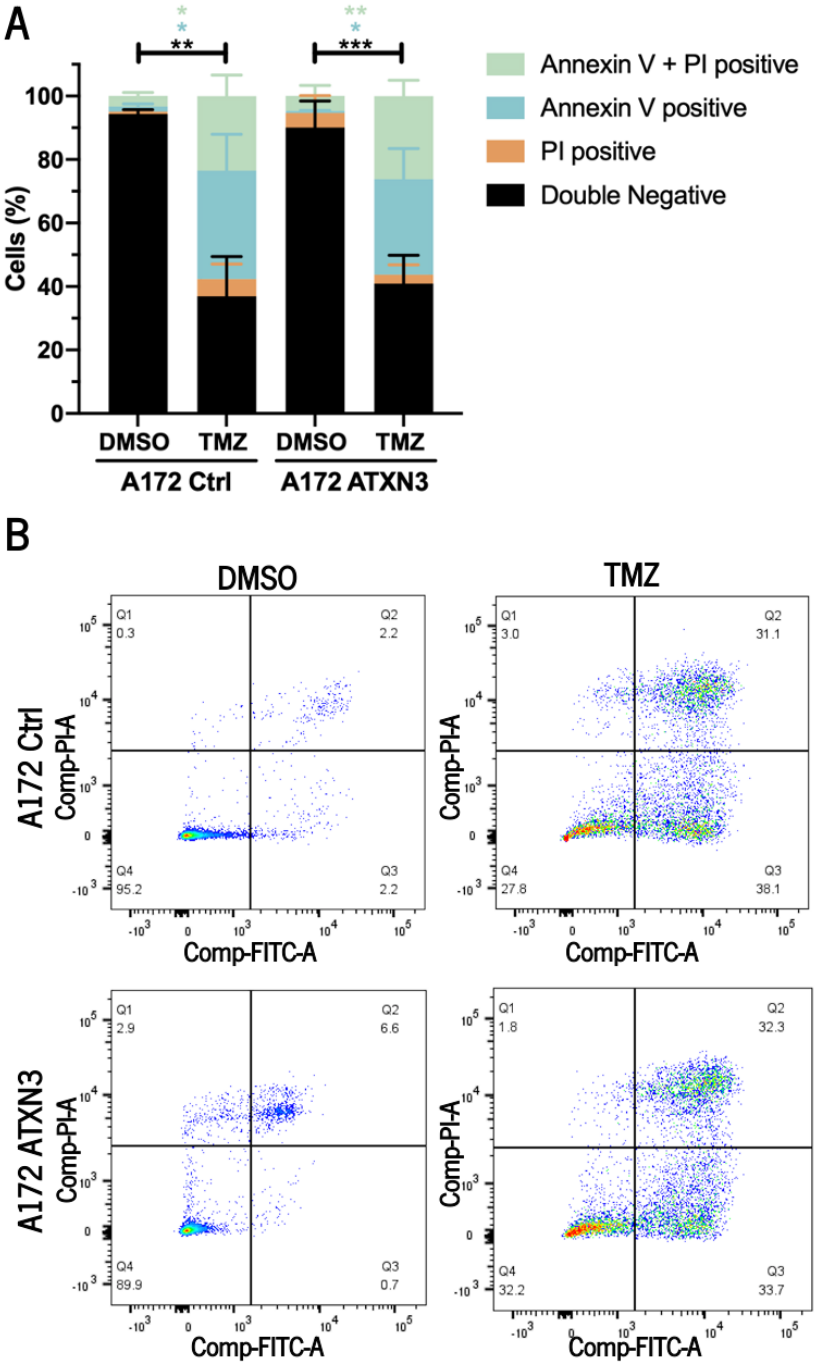

Figure 10. ATXN3 does not affect the sensitivity of GBM cells to TMZ. (A-B) A172-ATXN3 and A172-Ctrl cells were treated with DMSO (vehicle) or TMZ for 6 days and cell death was measured by flow cytometry (n=3). (A) Percentage of living and dead cells, labeled with Annexin V and PI. (B) Representative dot plots. *, $p < 0.05$; **, $p < 0.01$ and ***, $p < 0.001$ (two-way ANOVA post-hoc Tukey test). DMSO: dimethyl sulfoxide; PI: propidium iodide; TMZ: temozolomide.

4.5 *ATXN3* has prognostic value in GBM patients

Given that our results suggest that ATXN3 plays a relevant role in GBM aggressiveness *in vitro* (**Figure 9**), we questioned whether in the clinical context there would be an association between *ATXN3* expression and the prognosis of GBM patients. To understand that we assessed the prognostic value of *ATXN3* expression in 573 GBM patients with survival data available in the TCGA database. According to the results, patients whose tumors have low *ATXN3* expression presented a statistically shorter OS (OS median of 13.9 months) compared to patients whose tumors have high levels of *ATXN3* expression (OS median of 15.4 months; $p = 0.0215$; Log-rank test; **Figure 11A**). Additionally, we validated the previous result in 8 additional independent datasets. This observation was consistent among 5 different datasets (Rembrandt, $p = 0.0074$, **Figure 11B**; Phillips, $p = 0.0475$, **Figure 11C**; Freije, $p = 0.0240$, **Figure 11D**; Vital, $p = 0.0002$, **Figure 11E**; and Joo, $p = 0.0072$, **Figure 11F**), and a similar trend was observed in the other 3 datasets (Gravendeel, $p = 0.0625$, **Figure 11G**; LeeY, $p = 0.0673$, **Figure 11H**; and Nutt, $p = 0.1060$, **Figure 11I**).

In addition to univariate analysis, a multivariate Cox analysis was performed using data from the TCGA database. This Cox model allows the use of *ATXN3* expression as a continuous variable and was used to take into account the potential confounding effect of other known prognostic factors such as patient age, KPS and gender. Interestingly, we observed a statistically significant association between lower *ATXN3* expression values and shorter OS in GBM patients ($p = 0.025$, Exp(B) = 0.713) independently of other prognostic factors (**Table 3**). As expected, increasing patient's age at diagnosis was significantly associated with worse OS ($p < 0.0001$, Exp(B) = 1.708) and increased KPS associated with better prognosis ($p < 0.0001$, Exp(B) = 0.976). GBM patient gender was not significantly associated with OS ($p = 0.085$).

We also performed a meta-analysis to systematically evaluate all datasets used and reinforce the association between *ATXN3* expression and the prognosis of GBM patients. Overall, the results demonstrate that high *ATXN3* expression is significantly associated with a better prognosis in GBM patients (HR = 0.612, 95% CI 0.506 – 0.739; $p < 0.0001$; random effect; **Figure 11J**).

Altogether, our findings show that *ATXN3* expression is associated with longer overall survival, establishing *ATXN3* as a clinically relevant biomarker of prognosis in GBM patients.

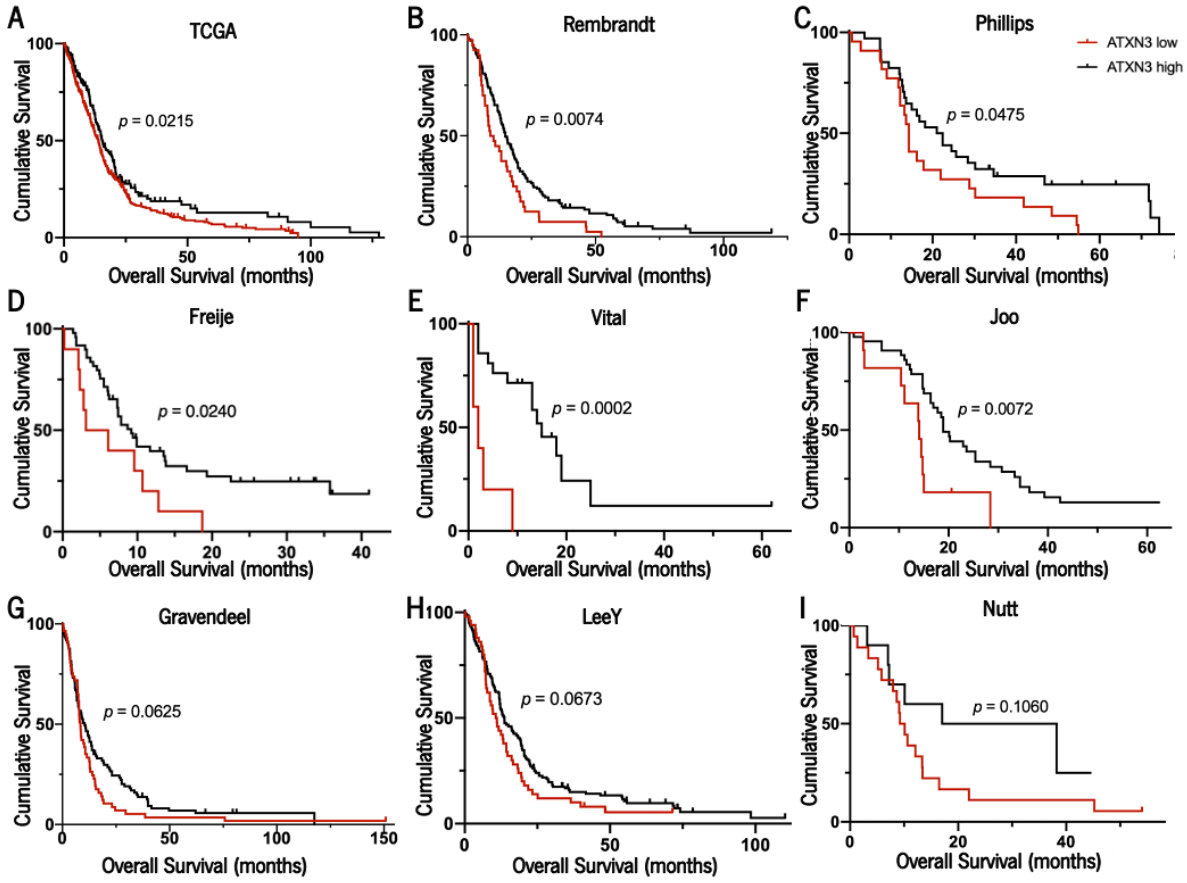

		TCGA	Rembrandt	Phillips	Freije	Vital	Joo	Gravendeel	LeeY	Nutt
ATXN3 expression	low	386	47	22	10	5	11	58	50	18
	high	187	156	34	49	21	43	101	141	10

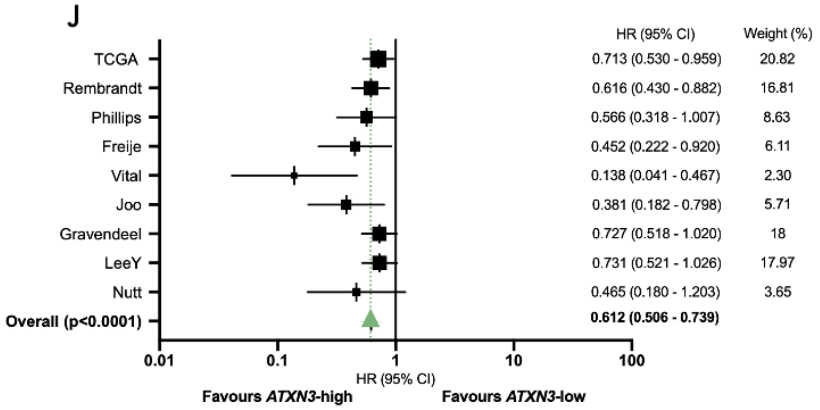

Figure 11. ATXN3 expression has a prognostic value in GBM patients. (A-I) Kaplan-Meier survival curves of GBM patients derived from **(A)** TCGA (n=573), **(B)** Rembrandt (n=203), **(C)** Phillips (n=56), **(D)** Freije (n=59), **(E)** Vital (n=26), **(F)** Joo (n=54), **(G)** Gravendeel (n=159), **(H)** LeeY (n=191) and **(I)** Nutt (n=28) datasets. **(J)** Meta-analysis with the association between ATXN3 expression and overall survival in patients with GBM. The size of each square represents the weight of the dataset in the meta-analysis and triangle is the combined effect. HR: hazard ratio, CI: confidence interval.

Table 3. Multivariate analysis of the association of *ATXN3* expression and survival of GBM patients, adjusted for patient age, KPS, and gender.

	Overall Survival		
	p-value	Exp(B)	95% CI
***ATXN3* expression**	0.025	0.713	0.530 – 0.958
Age[a,b]	<0.0001	1.708	1.328 – 2.197
KPS	<0.0001	0.976	0.967 – 0.985
Gender[a,c]	0.085	0.807	0.632 – 1.030

[a] Age and Gender was used as categorical variables;
[b] <=60 (n=211) vs +61 (n=169);
[c] Male (n=234) vs Female (n=146).

5. | DISCUSSION

5. DISCUSSION

Glioblastoma (GBM) is the most common and malignant type of glioma in adults (Ostrom et al., 2020). During the last few years, several efforts have been made to understand the molecular mechanisms of GBM and develop new treatments. Nonetheless, the prognosis of GBM patients is still extremely poor, being approximately 15 months after diagnosis (Stupp et al., 2005). Thus, it is crucial to identify and use new molecular markers allowing for patient stratification and therapy improvement. ATXN3 is a protein involved in SCA3 disease, a neurodegenerative disease caused by a CAG repeat expansion within the coding region of the *ATXN3* gene (Kawaguchi et al., 1994; Takiyama et al., 1993). In addition to its involvement in the pathogenesis of SCA3, ATXN3 has been described to play oncogenic or tumor suppressor functions in a variety of tumor types (Auer et al., 2007; Ergun et al., 2020; Ge et al., 2015; Neves-Carvalho et al., 2015; Sacco et al., 2014; Shi et al., 2018; Song et al., 2021; Zeng et al., 2014; Zou et al., 2019). However, the impact of ATXN3 in gliomas, particularly in GBM, is completely unknown until now. Thus, the present study is the first attempt to evaluate the expression of *ATXN3* in glioma and its potential role in this malignant brain tumor.

Our data showed that *ATXN3* expression decreases with glioma grade, being less expressed in glioma grade IV (GBM) when compared to less malignant gliomas (grade I, II and III) and normal samples available at the TCGA database (**Figure 6**, left panels), suggesting that higher *ATXN3* expression is associated with lower glioma malignancy. This was validated in 6 additional independent cohorts from various world regions (**Figure 7**). Additionally, we found that *ATXN3* is less expressed in IDH-wildtype gliomas (worse prognosis) when compared to IDH-mutant gliomas and with 1p/19q co-deletion (better prognosis) (**Figure 6**, right panels). Thus, *ATXN3* expression seems to be associated with IDH mutation and 1p/19q codeletion – and therefore with a better outcome – which fits well with the results found regarding its distribution along glioma grades. Accordingly, a study has shown that ATXN3 expression is decreased in gastric cancer, where ATXN3 play a role as tumor suppressor gene, when compared to non-cancerous tissue (Zeng et al., 2014). In contrast, in testicular cancer, where ATXN3 play a role as oncogene, ATXN3 was shown to be significantly overexpressed in testicular cancer tissues compared to normal ones.

Next, we wanted to further explore the potential role of ATXN3 in GBM. To do so, the expression of ATXN3 was initially characterized in GBM cell lines and patient-derived cultures. All GBM cells tested presented ATXN3 expression at the mRNA and protein level (**Figure 8**). It should be noted that *ATXN3* expression is more heterogeneous among GBM cells at the mRNA level, in contrast to ATXN3 expression at the protein level, which is more homogeneous. However, the cell line showing the lowest levels of

ATXN3 expression was the same in both techniques (A172 cell line), but there was no agreement between the two approaches on which GBM cell presents higher expression levels of ATXN3. These differences found between mRNA and protein levels might be explained by the fact that they have different regulatory mechanisms. Indeed, the central dogma that "DNA generates RNA that generates proteins" is not as simplistic as that and mRNA levels do not always correlate with protein expression, due to post-transcriptional and post-translational regulation (He, 2019; Hewitt, 2020). Also, the degradation time of proteins and genes can be different (de Sousa Abreu et al., 2009). Moreover, we are using techniques with completely different resolutions, one is quantitative (the qPCR), while the other is semi-quantitative (WB), which may not allow the detection of smaller differences that might be identifiable through qPCR.

ATXN3 is the causative protein of SCA3, a motor neurodegenerative disease that results from the unstable expansion of this protein's CAGs (Kawaguchi et al., 1994). *ATXN3* has a polymorphic CAG trinucleotide repeat tract of variable length among individuals: the CAG repeat length varies from 11 to 37 in healthy people, whereas it varies from 62 to 84 in SCA3 patients (Lindblad et al., 1996; Maciel et al., 1995; Ranum et al., 1995). Auer et al. demonstrated that patients with familiar and sporadic chronic lymphocytic leukemia, despite expressing ATXN3 with a number of CAG repeats within normal range (non-expanded), had a statistically significant increase in the frequency of high-length CAG repeats at the *ATXN3* locus compared with control-matched population (Auer et al., 2007). Taking this into account, we decided to determine the number of CAG repeat of the GBM cell line used (A172 cell line) and one of the cell lines with the highest endogenous expression of ATXN3 (U87MG cell line). We observed that in both cell lines *ATXN3* has 11 CAG repeats, which is within the normal range (Maciel et al., 1995), suggesting that ATXN3 expansion may not be crucial in GBM. However, this data should be interpreted with care as only two GBM cell lines were tested. In the future it will be necessary to determine the size of the ATXN3 CAG tract in a larger number of GBM cell lines, as well as in patient tumors.

To assess the impact of ATXN3 in GBM we genetically manipulated the expression of *ATXN3* in the A172 cell line, to increase its expression. Subsequently, several cancer hallmarks were evaluated (**Figure 9 and Figure 10**). In general, ATXN3 had an impact on GBM, decreasing its aggressiveness and acting mostly as a tumor suppressor gene. We found that higher ATXN3 expression is associated with decreased GBM cell viability in the two methods used, in the Trypan Blue after 6 days of incubation and in the MTS assay (**Figure 9B and C**). Interestingly, in the Trypan Blue assay, after 4 days of incubation, no statistically significant difference was observed. In line with this, in lung cancer, in which ATXN3 is considered an oncogene, ATXN3 was shown to be associated with an increase in cell viability (Sacco et al., 2014). In oral squamous cell carcinoma, ATXN3 silencing reduced the cell viability of cisplatin-resistant cells (Song

et al., 2021). The same effect was seen in testicular cancer, where ATXN3 promoted cell viability, functioning as an oncogene. Interestingly, it was discovered that this ability of ATXN3 to promote testicular cancer cell viability was due to the suppression of PTEN expression and to the indirect activation of AKT/mTOR signaling pathway (Shi et al., 2018). This signaling pathway constituted an important pathway in cancer, including in GBM, and PTEN is a tumor suppressor that inhibits this pathway, helping to prevent cancer. As a result, the loss of PTEN function allows unrestricted AKT signaling, resulting in cell survival and tumor growth (Porta et al., 2014). In GBM, PTEN is frequently deleted due to mutations or loss of heterozygosity. This loss of PTEN plays a key role in the tumor's development and aggressive behavior, and, furthermore, it is correlated with poor survival in GBM patients (Koul, 2008). Thus, it will be important in the future to evaluate whether and how ATXN3 affects the expression of this tumor suppressor gene in GBM cells and/or it impacts the activation of the important PI3K/AKT/mTOR pathway; this can be achieved by assessing the expression of proteins related to the pathway. In our assays, ATXN3 did not affect cell proliferation (**Figure 9D**), nor cell cycle progression in GBM (**Figure 9E and F**), neither did it affect GBM cells' migration (**Figure 9G and H**). Of note, silencing ATXN3 in the neuroblastoma cell line resulted in a greater number of cells in S phase and significantly increased migratory capacity of the cells (Neves-Carvalho et al., 2015). On the other hand, in breast cancer, where ATXN3 was shown to have an oncogenic function, ATXN3 silencing significantly decreased cancer cell migration (Zou et al., 2019). Although GBMs rarely metastasize, they have a highly infiltrative behavior across the brain tissue. This important feature of GBM makes complete surgical resection impossible, resulting in a less effective treatment (So et al., 2021). Here, we found that higher ATXN3 expression is associated with a decreased invasion capacity of the GBM cell model (**Figure 9I and J**). In the clinical context, this association with a decreased invasion capacity may perhaps contribute to a more complete tumor resection and, consequently a better treatment outcome for GBM patients. Thus, this finding is in line with the fact that we show that *ATXN3* is a new positive biomarker for GBM, being associated with a better prognosis in patients with the disease (**Figure 11**). In breast cancer, where ATXN3 was considered an oncogene, its expression was associated with an increased invasive capacity of the cells, as expected, the opposite of what was observed by us in GBM (Zou et al., 2019). Although the precise biological function of ATXN3 remains largely unknown, it is known that ATXN3 acts as a deubiquitinating enzyme (DUB), regulating the deubiquitination and stability of various proteins (B. Burnett et al., 2003; Winborn et al., 2008). Of note, ATXN3 has been identified in breast cancer as the DUB of Krüppel-like factor 4 (KLF4), an important transcription factor. Indeed, the impact of ATXN3 on breast cancer cell migration and invasion was shown to be due to its regulation of KLF4 (Zou et al., 2019). Interestingly, studies have shown that KLF4 levels

are highly regulated in high-grade gliomas, including GBM (Elsir et al., 2014; Holmberg et al., 2011), and, KLF4 has been demonstrated to act as an oncogene in GBM (Ray, 2016). With this in mind, the question that arises is: might ATXN3's impact in reducing the aggressiveness of GBM cells be owing to the fact that it is acts as a DUB of KLF4 and lowering its expression levels and, therefore, preventing its oncogenic effect in GBM? In the future, it would be interesting to evaluate this, as well as verify if ATXN3's role in GBM is due to its function as a DUB but affecting other proteins. The inclusion of TMZ in the standard GBM treatment resulted in a significant improvement in patient survival of 2.3 months (Stupp et al., 2005). However, unfortunately, more than half of patients with GBM treated with TMZ are resistant to this agent and do not respond to therapy, which leads to an unsatisfactory clinical outcome (S. Y. Lee, 2016). Thus, in this study, we also evaluated whether ATXN3 could impact on TMZ-mediated cell death of GBM cells. We observed that TMZ treatment increased the number of apoptotic cells in both cell lines (A172-Ctrl and A172-ATXN3) compared to vehicle treatment (**Figure 10**). This result was expected, since TMZ has a cytotoxic effect on tumor cells resulting in cell death. However, ATXN3 did not affect the sensitivity of cells to TMZ when comparing ATXN3 overexpressing cells and control cells. Song et al., demonstrated that ATXN3 was responsible for the resistance of oral squamous cell carcinoma cells to cisplatin (Song et al., 2021). As we only performed these *in vitro* assays in one GBM cell line, in the future it will be important to validate the results in other GBM cell lines and also using an ATXN3-silencing model. In fact, we already infected U87MG cells (presenting high expression levels of ATXN3) with lentiviral particles containing the ATXN3-silencing vector or the respective scramble vector to obtain an ATXN3-silencing model. However, and despite several attempts, we were yet unable to successfully obtain and characterize this model. Also, we are planning to assess the impact of ATXN3 expression in the survival of an orthotopic GBM mouse model and to corroborate the results obtained *in vitro* and in patients (**Figure 11**). This expansion from *in vitro* to *in vivo* models is important as the latter allow reproducing the complex interactions between the tumor and the microenvironment, which is not possible to evaluate *in vitro*. For this, a matched pair of ATXN3-high and low GBM cells might be intracranially stereotactically injected in the brain striatum of NSG immunodeficient mice (NOD.Cg-Prkdc^{scid}/Il2tg^{tm1Wjl}/SzJ) and survival time might be evaluated. Furthermore, it will be interesting to perform cellular and molecular analysis: for example, to evaluate the tumor volume in all animals and to assess the levels of proliferation and cell death in the tumors, through immunohistochemistry of the collected brain and tumors.

GBMs are extremely heterogeneous tumors (Brandes et al., 2008). In order to stratify patients and improve therapy and prognosis, molecular markers of prognosis that are altered in a high percentage of patients, such as IDH mutations and the *MGMT* promoter methylation, have been identified (Szopa et al.,

2017; Xavier-Magalhães et al., 2013). Thus, we aimed to understand whether the *ATXN3* expression has a clinical value in GBM and can help in the stratification of GBM patients that have a poor prognosis and low survival rates. For this we used several publicly available datasets and found that *ATXN3* was associated with longer overall survival of GBM patients (**Figure 11**). This association between *ATXN3* and GBM patient overall survival was also assessed independently of other well-characterized prognostic factors in GBM, such as patient age, KPS and gender, where the same statistically significant result was found (**Table 3**). Thus, we show that *ATXN3* is a novel positive prognostic biomarker in GBM. These findings support the role of ATXN3 as a tumor suppressor gene as suggested by our *in* vitro studies (**Figure 9**). Furthermore, they add up to the fact that *ATXN3* levels decrease as glioma malignancy progresses (from grade I to grade IV glioma) and are linked to the IDH mutation and 1p/19q codeletion gliomas, the subtypes with the best prognostic outcome (**Figure 6 and Figure 7**). Notably, *ATXN3* was also found to have prognostic value in breast cancer, where it acts as an oncogene, being associated with a patients' poor prognosis (Zou et al., 2019). In familiar and sporadic chronic lymphocytic leukemia, *ATXN3* was also associated with disease prognosis. Interestingly, the authors found that high-length CAG repeats in *ATXN3* were also associated with poor prognosis (Auer et al., 2007). Furthermore, in testicular cancer, ATXN3 expression levels were found to be positively correlated with disease stage and metastasis, with higher ATXN3 expression being associated with more advanced disease stages (stage II and III) and a higher number of metastases (3 or more metastases) (Shi et al., 2018). In renal cell carcinoma, *ATXN3* levels were significantly higher in Fuhrman grade 4 (usually with worse prognosis) than in other grades (Ergun et al., 2020).

In gastric cancer, ATXN3 expression has been found to be positively correlated with p53 protein expression (Zeng et al., 2014). In GBM, the TP53 gene, which encodes the p53 protein, is frequently mutated. p53 plays an important role as a tumor suppressor and is considered the "guardian of the genome", playing a role in cell cycle control, apoptosis and promoting DNA repair processes (Y. Zhang et al., 2018). In the future, it will be important to assess whether ATXN3 expression is associated with p53 in GBM and whether its role in GBM has anything to do with this possible association.

To date, there is no effective treatment for SCA3, a progressive and fatal disease. Recently, gene therapy aimed at silencing ATXN3 expression emerged as a new potential therapeutic strategy for SCA3 (reviewed by Neves-Carvalho et al., 2020). Studies have shown that in wild-type and SCA3 rodent models silencing of ATXN3 allele improved the observed neuropathology, decreasing neuropathological abnormalities and/or motor deficits (Alves et al., 2008, 2010; Nóbrega et al., 2013; Rodríguez-Lebrón et al., 2013). While promising, it is critical to assess the long-term side effects of chronically decreasing

ATXN3 levels before moving to the clinical trials, since ATXN3 has been implicated on several types of cancer (Auer et al., 2007; Ergun et al., 2020; Ge et al., 2015; Neves-Carvalho et al., 2015; Sacco et al., 2014; Shi et al., 2018; Song et al., 2021; Zeng et al., 2014; Zou et al., 2019). Indeed, here we showed that ATXN3 may play a role as a tumor suppressor gene in GBM. Therefore, it is critical to assess the tumorigenic potential of ATXN3 to initiate intracranial growth of gliomas, as it was previously performed for other genes (Pojo et al., 2015; Sonoda et al., 2001). One way to study this is using non-tumorigenic immortalized astrocytes (e.g., hTERT/E6/E7) (Tsuruga et al., 2008), which express ATXN3 (**Figure 8**) that would be silenced in these cells and their tumorigenic potential would be evaluated after injection into the brain of immunocompromised mice (e.g., NSG).

6. | CONCLUSION

6. CONCLUSIONS

This work was the first to assess the role of ATXN3 in gliomas, particularly in GBM, the most malignant one.

We demonstrated that *ATXN3* expression levels decrease with glioma grade and consequently with its malignancy, being less expressed in GBM (grade IV glioma) when compared to lower-grade gliomas and normal samples. Additionally, in a more in-depth study on GBM, we found that ATXN3 is differentially expressed in several GBM cells, both at the protein and mRNA level. We found that ATXN3 impacts some cancer hallmarks *in vitro*, acting mostly as a tumor suppressor gene. Finally, and very importantly, *ATXN3* expression was shown to be associated with a longer overall survival of GBM patients, demonstrating that ATXN3 can be a new positive prognostic factor in GBM.

Although more studies are needed in the future to confirm our results, here we described for the first time the role of ATXN3 in GBM, suggesting that it plays a role as a tumor suppressor gene in this malignant cancer, and demonstrating that ATXN3 is a positive prognostic factor in GBM.

7. | REFERENCES

7. REFERENCES

Ahlbom, A., Feychting, M., Green, A., Kheifets, L., Savitz, D. A., & Swerdlow, A. J. (2009). Epidemiologic evidence on mobile phones and tumor risk: A review. *Epidemiology*, *20*(5), 639–652. https://doi.org/10.1097/EDE.0b013e3181b0927d

Ahmadloo, N., Kani, A. A., Mohammadianpanah, M., Nasrolahi, H., Omidvari, S., Mosalaei, A., & Ansari, M. (2013). Treatment outcome and prognostic factors of adult glioblastoma multiforme. *Journal of the Egyptian National Cancer Institute*, *25*(1), 21–30. https://doi.org/10.1016/j.jnci.2012.11.001

Almeida, B., Abreu, I. A., Matos, C. A., Fraga, J. S., Fernandes, S., Macedo, M. G., Gutiérrez-Gallego, R., Pereira, P. J. B., Carvalho, A. L., & Macedo-Ribeiro, S. (2015). SUMOylation of the brain-predominant Ataxin-3 isoform modulates its interaction with p97. *Biochimica et Biophysica Acta - Molecular Basis of Disease*, *1852*(9), 1950–1959. https://doi.org/10.1016/j.bbadis.2015.06.010

Alves, S., Nascimento-Ferreira, I., Auregan, G., Hassig, R., Dufour, N., Brouillet, E., Pedroso de Lima, M. C., Hantraye, P., de Almeida, L. P., & Déglon, N. (2008). Allele-specific RNA silencing of mutant ataxin-3 mediates neuroprotection in a rat model of Machado-Joseph disease. *PLoS ONE*, *3*(10). https://doi.org/10.1371/journal.pone.0003341

Alves, S., Nascimento-Ferreira, I., Dufour, N., Hassig, R., Auregan, G., Nóbrega, C., Brouillet, E., Hantraye, P., Pedroso de Lima, M. C., Déglon, N., & de Almeida, L. P. (2010). Silencing ataxin-3 mitigates degeneration in a rat model of Machado-Joseph disease: No role for wild-type ataxin-3? *Human Molecular Genetics*, *19*(12), 2380–2394. https://doi.org/10.1093/hmg/ddq111

Antony, P. M. A., Mäntele, S., Mollenkopf, P., Boy, J., Kehlenbach, R. H., Riess, O., & Schmidt, T. (2009). Identification and functional dissection of localization signals within ataxin-3. *Neurobiology of Disease*, *36*(2), 280–292. https://doi.org/10.1016/j.nbd.2009.07.020

Auer, R. L., Dighiero, G., Goldin, L. R., Syndercombe-Court, D., Jones, C., McElwaine, S., Newland, A. C., Fegan, C. D., Caporaso, N., & Cotter, F. E. (2007). Trinucleotide repeat dynamic mutation identifying susceptibility in familial and sporadic chronic lymphocytic leukaemia. *British Journal of Haematology*, *136*(1), 73–79. https://doi.org/10.1111/j.1365-2141.2006.06388.x

Benson, V. S., Pirie, K., Schüz, J., Reeves, G. K., Beral, V., & Green, J. (2013). Mobile phone use and risk of brain neoplasms and other cancers: prospective study. *International Journal of Epidemiology*, *42*(3), 792–802. https://doi.org/10.1093/ije/dyt072

Berke, S. J. S., Chai, Y., Marrs, G. L., Wen, H., & Paulson, H. L. (2005). Defining the role of ubiquitin-interacting motifs in the polyglutamine disease protein, ataxin-3. *Journal of Biological Chemistry*, *280*(36), 32026–32034. https://doi.org/10.1074/jbc.M506084200

Bettencourt, C., Santos, C., Montiel, R., Do Carmo Costa, M., Cruz-Morales, P., Santos, L. R., Simões, N., Kay, T., Vasconcelos, J., Maciel, P., & Lima, M. (2010). Increased transcript diversity: Novel splicing variants of Machado-Joseph Disease gene (ATXN3). *Neurogenetics*, *11*(2), 193–202. https://doi.org/10.1007/s10048-009-0216-y

Bowman, R. L., Wang, Q., Carro, A., Verhaak, R. G. W., & Squatrito, M. (2017). GlioVis data portal for visualization and analysis of brain tumor expression datasets. *Neuro-Oncology*, *19*(1), 139–141. https://doi.org/10.1093/neuonc/now247

Braganza, M. Z., Kitahara, C. M., Berrington De González, A., Inskip, P. D., Johnson, K. J., & Rajaraman,

P. (2012). Ionizing radiation and the risk of brain and central nervous system tumors: A systematic review. *Neuro-Oncology*, *14*(11), 1316–1324. https://doi.org/10.1093/neuonc/nos208

Brait, M., & Sidransky, D. (2011). Cancer epigenetics: Above and beyond. *Toxicology Mechanisms and Methods*, *21*(4), 275–288. https://doi.org/10.3109/15376516.2011.562671

Brandes, A. A., Tosoni, A., Franceschi, E., Reni, M., Gatta, G., & Vecht, C. (2008). Glioblastoma in adults. *Critical Reviews in Oncology/Hematology*, *67*(2), 139–152. https://doi.org/10.1016/j.critrevonc.2008.02.005

Bray, F., Laversanne, M., Weiderpass, E., & Soerjomataram, I. (2021). The ever-increasing importance of cancer as a leading cause of premature death worldwide. *Cancer*, *127*(16), 3029–3030. https://doi.org/10.1002/cncr.33587

Buckner, J. C., Brown, P. D., O'Neill, B. P., Meyer, F. B., Wetmore, C. J., & Uhm, J. H. (2007). Central nervous system tumors. *Mayo Clinic Proceedings*, *82*(10), 1271–1286. https://doi.org/10.4065/82.10.1271

Burnet, N. G., Jefferies, S. J., Benson, R. J., Hunt, D. P., & Treasure, F. P. (2005). Years of life lost (YLL) from cancer is an important measure of population burden - And should be considered when allocating research funds. *British Journal of Cancer*, *92*(2), 241–245. https://doi.org/10.1038/sj.bjc.6602321

Burnett, B. G., & Pittman, R. N. (2005). The polyglutamine neurodegenerative protein ataxin 3 regulates aggresome formation. *Proceedings of the National Academy of Sciences of the United States of America*, *102*(12), 4330–4335. https://doi.org/10.1073/pnas.0407252102

Burnett, B., Li, F., & Pittman, R. N. (2003). The polyglutamine neurodegenerative protein ataxin-3 binds polyubiquitylated proteins and has ubiquitin protease activity. *Human Molecular Genetics*, *12*(23), 3195–3205. https://doi.org/10.1093/hmg/ddg344

Cairncross, G., & Jenkins, R. (2008). Gliomas With 1p/19q Codeletion:a.k.a. Oligodendroglioma. *The Cancer Journal*, *14*(6), 352–357. https://doi.org/10.1097/PPO.0b013e31818d8178

Carvalho, A. L., Silva, A., & Macedo-Ribeiro, S. (2018). *Polyglutamine-Independent Features in Ataxin-3 Aggregation and Pathogenesis of Machado-Joseph Disease* (pp. 275–288). https://doi.org/10.1007/978-3-319-71779-1_14

Chai, Y., Berke, S. S., Cohen, R. E., & Paulson, H. L. (2004). Poly-ubiquitin Binding by the Polyglutamine Disease Protein Ataxin-3 Links Its Normal Function to Protein Surveillance Pathways. *Journal of Biological Chemistry*, *279*(5), 3605–3611. https://doi.org/10.1074/jbc.M310939200

Chen, H., Ward, M. H., Tucker, K. L., Graubard, B. I., McComb, R. D., Potischman, N. A., Weisenburger, D. D., & Heineman, E. F. (2002). Diet and risk of adult glioma in eastern Nebraska, United States. *Cancer Causes and Control*, *13*(7), 647–655. https://doi.org/10.1023/A:1019527225197

Chow, M. K. M., MacKay, J. P., Whisstock, J. C., Scanlon, M. J., & Bottomley, S. P. (2004). Structural and functional analysis of the Josephin domain of the polyglutamine protein ataxin-3. *Biochemical and Biophysical Research Communications*, *322*(2), 387–394. https://doi.org/10.1016/j.bbrc.2004.07.131

Clarke, J., Butowski, N., & Chang, S. (2010). Recent Advances in Therapy for Glioblastoma. *Archives of Neurology*, *67*(3). https://doi.org/10.1001/archneurol.2010.5

Coble, J. B., Dosemeci, M., Stewart, P. A., Blair, A., Bowman, J., Fine, H. A., Shapiro, W. R., Selker, R. G., Loeffler, J. S., Black, P. M., Linet, M. S., & Inskip, P. D. (2009). Occupational exposure to

magnetic fields and the risk of brain tumors. *Neuro-Oncology*, *11*(3), 242–249. https://doi.org/10.1215/15228517-2009-002

Cohen, A. L., Holmen, S. L., & Colman, H. (2013). IDH1 and IDH2 Mutations in Gliomas. *Current Neurology and Neuroscience Reports*, *13*(5), 345. https://doi.org/10.1007/s11910-013-0345-4

Costa, M. do C., Bajanca, F., Rodrigues, A.-J., Tomé, R. J., Corthals, G., Macedo-Ribeiro, S., Paulson, H. L., Logarinho, E., & Maciel, P. (2010). Ataxin-3 Plays a Role in Mouse Myogenic Differentiation through Regulation of Integrin Subunit Levels. *PLoS ONE*, *5*(7), e11728. https://doi.org/10.1371/journal.pone.0011728

Cunha, M. L. V. da, & Maldaun, M. V. C. (2019). Metastasis from glioblastoma multiforme: a meta-analysis. *Revista Da Associação Médica Brasileira*, *65*(3), 424–433. https://doi.org/10.1590/1806-9282.65.3.424

Dang, L., White, D. W., Gross, S., Bennett, B. D., Bittinger, M. A., Driggers, E. M., Fantin, V. R., Jang, H. G., Jin, S., Keenan, M. C., Marks, K. M., Prins, R. M., Ward, P. S., Yen, K. E., Liau, L. M., Rabinowitz, J. D., Cantley, L. C., Thompson, C. B., Vander Heiden, M. G., … Su, M. (2009). Cancer-associated IDH1 mutations produce 2-hydroxyglutarate. *Nature*, *462*(7274), 739. https://doi.org/10.1038/nature08617.Cancer-associated

de Sousa Abreu, R., Penalva, L. O., Marcotte, E. M., & Vogel, C. (2009). Global signatures of protein and mRNA expression levels. *Molecular BioSystems*. https://doi.org/10.1039/b908315d

Djalilian, H. R., Shah, M. V., & Hall, W. A. (1999). Radiographic incidence of multicentric malignant gliomas. *Surgical Neurology*, *51*(5), 554–558. https://doi.org/10.1016/S0090-3019(98)00054-8

Do Carmo Costa, M., Gomes-Da-Silva, J., Miranda, C. J., Sequeiros, J., Santos, M. M., & Maciel, P. (2004). Genomic structure, promoter activity, and developmental expression of the mouse homologue of the Machado-Joseph disease (MJD) gene. *Genomics*, *84*(2), 361–373. https://doi.org/10.1016/j.ygeno.2004.02.012

Elsamadicy, A. A., Babu, R., Kirkpatrick, J. P., & Adamson, D. C. (2015). Radiation-induced malignant gliomas: A current review. *World Neurosurgery*, *83*(4), 530–542. https://doi.org/10.1016/j.wneu.2014.12.009

Elsir, T., Edqvist, P., Carlson, J., Ribom, D., Bergqvist, M., Ekman, S., Popova, S. N., Alafuzoff, I., Ponten, F., Nistér, M., & Smits, A. (2014). A study of embryonic stem cell-related proteins in human astrocytomas: Identification of Nanog as a predictor of survival. *International Journal of Cancer*, *134*(5), 1123–1131. https://doi.org/10.1002/ijc.28441

Ergun, S., Gunes, S., Buyukalpelli, R., & Aydin, O. (2020). Association of Abl interactor 2, ABI2, with platelet/lymphocyte ratio in patients with renal cell carcinoma: A pilot study. *International Journal of Experimental Pathology*, *101*(3–4), 87–95. https://doi.org/10.1111/iep.12349

Esteller, M., Garcia-Foncillas, J., Andion, E., Goodman, S. N., Hidalgo, O. F., Vanaclocha, V., Baylin, S. B., & Herman, J. G. (2000). Inactivation of the DNA-Repair Gene MGMT and the Clinical Response of Gliomas to Alkylating Agents. *New England Journal of Medicine*, *343*(19), 1350–1354. https://doi.org/10.1056/NEJM200011093431901

Evert, B. O., Araujo, J., Vieira-Saecker, A. M., De Vos, R. A. I., Harendza, S., Klockgether, T., & Wüllner, U. (2006). Ataxin-3 represses transcription via chromatin binding, interaction with histone deacetylase 3, and histone deacetylation. *Journal of Neuroscience*, *26*(44), 11474–11486. https://doi.org/10.1523/JNEUROSCI.2053-06.2006

Fayed, L. (2020). *Differentiating Between Primary and Metastatic Tumors*. https://www.verywellhealth.com/primary-and-metastatic-brain-tumors-513566

Feldheim, J., Kessler, A. F., Monoranu, C. M., Ernestus, R.-I., Löhr, M., & Hagemann, C. (2019). Changes of O6-Methylguanine DNA Methyltransferase (MGMT) Promoter Methylation in Glioblastoma Relapse—A Meta-Analysis Type Literature Review. *Cancers*, *11*(12), 1837. https://doi.org/10.3390/cancers11121837

Ferlay, J., Ervik, M., Lam, F., Colombet, M., Mery, L., Piñeros, M., Znaor, A., Soerjomataram, I., & Bray, F. (2020). *Global Cancer Observatory: Cancer Today*. Lyon, France: International Agency for Research on Cancer. https://gco.iarc.fr/today

Ferlay, J., Laversanne, M., Ervik, M., Lam, F., Colombet, M., Mery, L., Piñeros, M., Znaor, A., Soerjomataram, I., & Bray, F. (2020). *Global Cancer Observatory: Cancer Tomorrow*. Lyon, France: International Agency for Research on Cancer.

Fidler, M. M., Bray, F., & Soerjomataram, I. (2018). The global cancer burden and human development: A review. *Scandinavian Journal of Public Health*, *46*(1), 27–36. https://doi.org/10.1177/1403494817715400

Fraile, J. M., Quesada, V., Rodríguez, D., Freije, J. M. P., & López-Otín, C. (2012). Deubiquitinases in cancer: New functions and therapeutic options. *Oncogene*, *31*(19), 2373–2388. https://doi.org/10.1038/onc.2011.443

Freije, W. A., Castro-Vargas, F. E., Fang, Z., Horvath, S., Cloughesy, T., Liau, L. M., Mischel, P. S., & Nelson, S. F. (2004). Gene expression profiling of gliomas strongly predicts survival. *Cancer Research*, *64*(18), 6503–6510. https://doi.org/10.1158/0008-5472.CAN-04-0452

Ge, F., Chen, W., Qin, J., Zhou, Z., Liu, R., Liu, L., Tan, J., Zou, T., Li, H., Ren, G., & Chen, C. (2015). Ataxin-3 like (ATXN3L), a member of the Josephin family of deubiquitinating enzymes, promotes breast cancer proliferation by deubiquitinating Krüppel-like factor 5 (KLF5). *Oncotarget*, *6*(25), 21369–21378. https://doi.org/10.18632/oncotarget.4128

Gonçalves, C. S., Xavier-Magalhães, A., Martins, E. P., Pinto, A. A., Pires, M. M., Pinheiro, C., Reis, R. M., Sousa, N., & Costa, B. M. (2020). A novel molecular link between HOXA9 and WNT6 in glioblastoma identifies a subgroup of patients with particular poor prognosis. *Molecular Oncology*, *14*(6), 1224–1241. https://doi.org/10.1002/1878-0261.12633

Goto, J., Watanabe, M., Ichikawa, Y., Yee, S. B., Ihara, N., Endo, K., Igarashi, S., Takiyama, Y., Gaspar, C., Maciel, P., Tsuji, S., Rouleau, G. A., & Kanazawa, I. (1997). Machado-Joseph disease gene products carrying different carboxyl termini. *Neuroscience Research*, *28*(4), 373–377. https://doi.org/10.1016/S0168-0102(97)00056-4

Gravendeel, L. A. M., Kouwenhoven, M. C. M., Gevaert, O., De Rooi, J. J., Stubbs, A. P., Duijm, J. E., Daemen, A., Bleeker, F. E., Bralten, L. B. C., Kloosterhof, N. K., De Moor, B., Eilers, P. H. C., Van Der Spek, P. J., Kros, J. M., Sillevis Smitt, P. A. E., Van Den Bent, M. J., & French, P. J. (2009). Intrinsic gene expression profiles of gliomas are a better predictor of survival than histology. *Cancer Research*, *69*(23), 9065–9072. https://doi.org/10.1158/0008-5472.CAN-09-2307

Grizzi, F., & Chiriva-Internati, M. (2006). Cancer: Looking for simplicity and finding complexity. *Cancer Cell International*, *6*, 1–7. https://doi.org/10.1186/1475-2867-6-4

Hanahan, D., & Weinberg, R. A. (2011). Hallmarks of cancer: The next generation. *Cell*, *144*(5), 646–674. https://doi.org/10.1016/j.cell.2011.02.013

Hanif, F., Muzaffar, K., Perveen, K., Malhi, S. M., & Simjee, S. U. (2017). Glioblastoma multiforme: A review of its epidemiology and pathogenesis through clinical presentation and treatment. *Asian Pacific Journal of Cancer Prevention*, *18*(1), 3–9. https://doi.org/10.22034/APJCP.2017.18.1.3

Harris, G. M., Dodelzon, K., Gong, L., Gonzalez-Alegre, P., & Paulson, H. L. (2010). Splice isoforms of the polyglutamine disease protein ataxin-3 exhibit similar enzymatic yet different aggregation properties. *PLoS ONE*, *5*(10). https://doi.org/10.1371/journal.pone.0013695

He, C. (2019). Special Issue on Regulating the Central Dogma. *Biochemistry*, *58*(5), 295–296. https://doi.org/10.1021/acs.biochem.9b00059

Hegde, A. N., & Upadhya, S. C. (2011). Role of ubiquitin–proteasome-mediated proteolysis in nervous system disease. *Biochimica et Biophysica Acta (BBA) - Gene Regulatory Mechanisms*, *1809*(2), 128–140. https://doi.org/10.1016/j.bbagrm.2010.07.006

Hegi, M. E., Diserens, A.-C., Godard, S., Dietrich, P.-Y., Regli, L., Ostermann, S., Otten, P., Van Melle, G., de Tribolet, N., & Stupp, R. (2004). Clinical Trial Substantiates the Predictive Value of O-6-Methylguanine-DNA Methyltransferase Promoter Methylation in Glioblastoma Patients Treated with Temozolomide. *Clinical Cancer Research*, *10*(6), 1871–1874. https://doi.org/10.1158/1078-0432.CCR-03-0384

Hegi, M. E., Diserens, A.-C., Gorlia, T., Hamou, M.-F., de Tribolet, N., Weller, M., Kros, J. M., Hainfellner, J. A., Mason, W., Mariani, L., Bromberg, J. E. C., Hau, P., Mirimanoff, R. O., Cairncross, J. G., Janzer, R. C., & Stupp, R. (2005). MGMT Gene Silencing and Benefit from Temozolomide in Glioblastoma . *New England Journal of Medicine*, *352*(10), 997–1003. https://doi.org/10.1056/nejmoa043331

Heir, R., Ablasou, C., Dumontier, E., Elliott, M., Fagotto-Kaufmann, C., & Bedford, F. K. (2006). The UBL domain of PLIC-1 regulates aggresome formation. *EMBO Reports*, *7*(12), 1252–1258. https://doi.org/10.1038/sj.embor.7400823

Hewitt, S. M. (2020). Negative Consequences of the Central Dogma. *Journal of Histochemistry and Cytochemistry*, *68*(11), 731. https://doi.org/10.1369/0022155420970927

Holmberg, J., He, X., Peredo, I., Orrego, A., Hesselager, G., Ericsson, C., Hovatta, O., Oba-Shinjo, S. M., Marie, S. K. N., Nistér, M., & Muhr, J. (2011). Activation of Neural and Pluripotent Stem Cell Signatures Correlates with Increased Malignancy in Human Glioma. *PLoS ONE*, *6*(3), e18454. https://doi.org/10.1371/journal.pone.0018454

Iacob, G., & Dinca, E. B. (2009). Current data and strategy in glioblastoma multiforme. *Journal of Medicine and Life*, *2*(4), 386–393.

Ichikawa, Y., Goto, J., Hattori, M., Toyoda, A., Ishii, K., Jeong, S. Y., Hashida, H., Masuda, N., Ogata, K., Kasai, F., Hirai, M., Maciel, P., Rouleau, G. A., Sakaki, Y., & Kanazawa, I. (2001). The genomic structure and expression of MJD, the Machado-Joseph disease gene. *Journal of Human Genetics*, *46*(7), 413–422. https://doi.org/10.1007/s100380170060

Jansen, M., Yip, S., & Louis, D. N. (2010). Molecular pathology in adult gliomas: diagnostic, prognostic, and predictive markers. *The Lancet Neurology*, *9*(7), 717–726. https://doi.org/10.1016/S1474-4422(10)70105-8

Jenkins, R. B., Blair, H., Ballman, K. V., Giannini, C., Arusell, R. M., Law, M., Flynn, H., Passe, S., Felten, S., Brown, P. D., Shaw, E. G., & Buckner, J. C. (2006). A t(1;19)(q10;p10) Mediates the Combined Deletions of 1p and 19q and Predicts a Better Prognosis of Patients with Oligodendroglioma. *Cancer*

Research, *66*(20), 9852–9861. https://doi.org/10.1158/0008-5472.CAN-06-1796

Joo, K. M., Kim, J., Jin, J., Kim, M., Seol, H. J., Muradov, J., Yang, H., Choi, Y. La, Park, W. Y., Kong, D. S., Lee, J. Il, Ko, Y. H., Woo, H. G., Lee, J., Kim, S., & Nam, D. H. (2013). Patient-Specific Orthotopic Glioblastoma Xenograft Models Recapitulate the Histopathology and Biology of Human Glioblastomas In Situ. *Cell Reports*, *3*(1), 260–273. https://doi.org/10.1016/j.celrep.2012.12.013

Kamoun, A., Idbaih, A., Dehais, C., Elarouci, N., Carpentier, C., Letouzé, E., Colin, C., Mokhtari, K., Jouvet, A., Uro-Coste, E., Martin-Duverneuil, N., Sanson, M., Delattre, J.-Y., Figarella-Branger, D., de Reyniès, A., & Ducray, F. (2016). Integrated multi-omics analysis of oligodendroglial tumours identifies three subgroups of 1p/19q co-deleted gliomas. *Nature Communications*, *7*(1), 11263. https://doi.org/10.1038/ncomms11263

Kawaguchi, Y., Okamoto, T., Taniwaki, M., Aizawa, M., Inoue, M., Katayama, S., Kawakami, H., Nakamura, S., Nishimura, M., Akiguchi, I., Kimura, J., Narumiya, S., & Kakizuka, A. (1994). CAG expansions in a novel gene for Machado-Joseph disease at chromosome 14q32.1. *Nature Genetics*, *8*(3), 221–228. https://doi.org/10.1038/ng1194-221

Koul, D. (2008). PTEN Signaling pathways in glioblastoma. *Cancer Biology & Therapy*, *7*(9), 1321–1325. https://doi.org/10.4161/cbt.7.9.6954

Lee, S. Y. (2016). Temozolomide resistance in glioblastoma multiforme. *Genes & Diseases*, *3*(3), 198–210. https://doi.org/10.1016/j.gendis.2016.04.007

Lee, Y., Scheck, A. C., Cloughesy, T. F., Lai, A., Dong, J., Farooqi, H. K., Liau, L. M., Horvath, S., Mischel, P. S., & Nelson, S. F. (2008). Gene expression analysis of glioblastomas identifies the major molecular basis for the prognostic benefit of younger age. *BMC Medical Genomics*, *1*(1), 1–12. https://doi.org/10.1186/1755-8794-1-52

Li, F., Macfarlan, T., Pittman, R. N., & Chakravarti, D. (2002). Ataxin-3 is a histone-binding protein with two independent transcriptional corepressor activities. *Journal of Biological Chemistry*, *277*(47), 45004–45012. https://doi.org/10.1074/jbc.M205259200

Lindblad, K., Lunkes, A., Maciel, P., Stevanin, G., Zander, C., Klockgether, T., Ratzlaff, T., Brice, A., Rouleau, G. A., Hudson, T., Auburger, G., & Schalling, M. (1996). Mutation detection in Machado-Joseph disease using repeat expansion detection. *Molecular Medicine*, *2*(1), 77–85. https://doi.org/10.1007/bf03402204

Linhartová, I., Repitz, M., Dráber, P., Nemec, M., Wiche, G., & Propst, F. (1999). Conserved domains and lack of evidence for polyglutamine length polymorphism in the chicken homolog of the Machado-Joseph disease gene product ataxin-3. *Biochimica et Biophysica Acta - Gene Structure and Expression*, *1444*(2), 299–305. https://doi.org/10.1016/S0167-4781(99)00004-4

Livak, K. J., & Schmittgen, T. D. (2001). Analysis of Relative Gene Expression Data Using Real-Time Quantitative PCR and the 2−ΔΔCT Method. *Methods*, *25*(4), 402–408. https://doi.org/10.1006/meth.2001.1262

Louis, D. N., Ohgaki, H., Wiestler, O. D., Cavenee, W. K., Burger, P. C., Jouvet, A., Scheithauer, B. W., & Kleihues, P. (2007). The 2007 WHO classification of tumours of the central nervous system. *Acta Neuropathologica*, *114*(2), 97–109. https://doi.org/10.1007/s00401-007-0243-4

Louis, D. N., Perry, A., Reifenberger, G., von Deimling, A., Figarella-Branger, D., Cavenee, W. K., Ohgaki, H., Wiestler, O. D., Kleihues, P., & Ellison, D. W. (2016). The 2016 World Health Organization

Classification of Tumors of the Central Nervous System: a summary. *Acta Neuropathologica*, *131*(6), 803–820. https://doi.org/10.1007/s00401-016-1545-1

Louis, D. N., Perry, A., Wesseling, P., Brat, D. J., Cree, I. A., Figarella-Branger, D., Hawkins, C., Ng, H. K., Pfister, S. M., Reifenberger, G., Soffietti, R., Von Deimling, A., & Ellison, D. W. (2021). The 2021 WHO classification of tumors of the central nervous system: A summary. *Neuro-Oncology*, *23*(8), 1231–1251. https://doi.org/10.1093/neuonc/noab106

Lukas, R. V, Wainwright, D. A., Ladomersky, E., Sachdev, S., Sonabend, A. M., & Stupp, R. (2019). Newly Diagnosed Glioblastoma: A Review on Clinical Management. *Oncology (Williston Park, N.Y.)*, *33*(3), 91–100. http://www.ncbi.nlm.nih.gov/pubmed/30866031

Macedo-Ribeiro, S., Cortes, L., Maciel, P., & Carvalho, A. L. (2009). Nucleocytoplasmic Shuttling Activity of Ataxin-3. *PLoS ONE*, *4*(6), e5834. https://doi.org/10.1371/journal.pone.0005834

Maciel, P., Gaspar, C., DeStefano, A. L., Silveira, I., Coutinho, P., Radvany, J., Dawson, D. M., Sudarsky, L., Guimaraes, J., Loureiro, J. E. L., Nezarati, M. M., Corwin, L. I., Lopes-Cendes, I., Rooke, K., Rosenberg, R., MacLeod, P., Farrer, L. A., Sequeiros, J., & Rouleau, G. A. (1995). Correlation between CAG repeat length and clinical features in Machado- Joseph disease. *American Journal of Human Genetics*, *57*(1), 54–61.

Madhavan, S., Zenklusen, J. C., Kotliarov, Y., Sahni, H., Fine, H. A., & Buetow, K. (2009). Rembrandt: Helping personalized medicine become a reality through integrative translational research. *Molecular Cancer Research*, *7*(2), 157–167. https://doi.org/10.1158/1541-7786.MCR-08-0435

Mao, Y., Senic-Matuglia, F., Di Fiore, P. P., Polo, S., Hodsdon, M. E., & De Camilli, M. (2005). Deubiquitinating function of ataxin-3: Insights from the solution structure of the Josephin domain. *Proceedings of the National Academy of Sciences of the United States of America*, *102*(36), 12700–12705. https://doi.org/10.1073/pnas.0506344102

Masino, L., Musi, V., Menon, R. P., Fusi, P., Kelly, G., Frenkiel, T. A., Trottier, Y., & Pastore, A. (2003). Domain architecture of the polyglutamine protein ataxin-3: A globular domain followed by a flexible tail. *FEBS Letters*, *549*(1–3), 21–25. https://doi.org/10.1016/S0014-5793(03)00748-8

Masui, K., Mischel, P. S., & Reifenberger, G. (2016). Molecular classification of gliomas. In *Handbook of Clinical Neurology* (1st ed., Vol. 134). Elsevier B.V. https://doi.org/10.1016/B978-0-12-802997-8.00006-2

Matos, C. A., de Almeida, L. P., & Nóbrega, C. (2019). Machado–Joseph disease/spinocerebellar ataxia type 3: lessons from disease pathogenesis and clues into therapy. *Journal of Neurochemistry*, *148*(1), 8–28. https://doi.org/10.1111/jnc.14541

Matos, C. A., de Macedo-Ribeiro, S., & Carvalho, A. L. (2011). Polyglutamine diseases: The special case of ataxin-3 and Machado-Joseph disease. *Progress in Neurobiology*, *95*(1), 26–48. https://doi.org/10.1016/j.pneurobio.2011.06.007

Matos, C. A., Nóbrega, C., Louros, S. R., Almeida, B., Ferreiro, E., Valero, J., De Almeida, L. P., Macedo-Ribeiro, S., & Carvalho, A. L. (2016). Ataxin-3 phosphorylation decreases neuronal defects in spinocerebellar ataxia type 3 models. *Journal of Cell Biology*, *212*(4), 465–480. https://doi.org/10.1083/jcb.201506025

Mueller, T., Breuer, P., Schmitt, I., Walter, J., Evert, B. O., & Wüllner, U. (2009). CK2-dependent phosphorylation determines cellular localization and stability of ataxin-3. *Human Molecular Genetics*, *18*(17), 3334–3343. https://doi.org/10.1093/hmg/ddp274

Neves-Carvalho, A., Duarte-Silva, S., Silva, J., Almeida, B., Heetveld, S., Sotiropoulos, I., Heutink, P., Li, K. W., & Maciel, P. (2019). Regulation of neuronal mRNA splicing and Tau isoform ratio by ATXN3 through deubiquitylation of splicing factors. *BioRxiv*, 711424. https://doi.org/10.1101/711424

Neves-Carvalho, A., Duarte-Silva, S., Teixeira-Castro, A., & Maciel, P. (2020). Polyglutamine spinocerebellar ataxias: emerging therapeutic targets. *Expert Opinion on Therapeutic Targets*, *0*(0). https://doi.org/10.1080/14728222.2020.1827394

Neves-Carvalho, A., Logarinho, E., Freitas, A., Duarte-Silva, S., do Carmo Costa, M., Silva-Fernandes, A., Martins, M., Serra, S. C., Lopes, A. T., Paulson, H. L., Heutink, P., Relvas, J. B., & Maciel, P. (2015). Dominant negative effect of polyglutamine expansion perturbs normal function of ataxin-3 in neuronal cells. *Human Molecular Genetics*, *24*(1), 100–117. https://doi.org/10.1093/hmg/ddu422

Nicastro, G., Menon, R. P., Masino, L., Knowles, P. P., McDonald, N. Q., & Pastore, A. (2005). The solution structure of the Josephin domain of ataxin-3: Structural determinants for molecular recognition. *Proceedings of the National Academy of Sciences of the United States of America*, *102*(30), 10493–10498. https://doi.org/10.1073/pnas.0501732102

Nóbrega, C., Nascimento-Ferreira, I., Onofre, I., Albuquerque, D., Hirai, H., Déglon, N., & de Almeida, L. P. (2013). Silencing Mutant Ataxin-3 Rescues Motor Deficits and Neuropathology in Machado-Joseph Disease Transgenic Mice. *PLoS ONE*, *8*(1). https://doi.org/10.1371/journal.pone.0052396

Nutt, C. L., Mani, D. R., Betensky, R. A., Tamayo, P., Cairncross, J. G., Ladd, C., Pohl, U., Hartmann, C., McLaughlin, M. E., Batchelor, T. T., Black, P. M., Von Deimling, A., Pomeroy, S. L., Golub, T. R., & Louis, D. N. (2003). Gene expression-based classification of malignant gliomas correlates better with survival than histological classification. *Cancer Research*, *63*(7), 1602–1607.

Ohgaki, H., & Kleihues, P. (2013). The definition of primary and secondary glioblastoma. *Clinical Cancer Research*, *19*(4), 764–772. https://doi.org/10.1158/1078-0432.CCR-12-3002

Omuro, A., & DeAngelis, L. M. (2013). Glioblastoma and other malignant gliomas: A clinical review. *JAMA - Journal of the American Medical Association*, *310*(17), 1842–1850. https://doi.org/10.1001/jama.2013.280319

Ostrom, Q. T., Gittleman, H., Stetson, L., Virk, S., & Barnholtz-Sloan, J. S. (2017). Epidemiology of Intracranial Gliomas. *Progress in Neurological Surgery*, *30*, 1–11. https://doi.org/10.1159/000464374

Ostrom, Q. T., Patil, N., Cioffi, G., Waite, K., Kruchko, C., & Barnholtz-Sloan, J. S. (2020). CBTRUS statistical report: Primary brain and other central nervous system tumors diagnosed in the United States in 2013-2017. *Neuro-Oncology*, *22*(Supplement_1), IV1–IV96. https://doi.org/10.1093/neuonc/noaa200

Parsons, D. W., Jones, S., Zhang, X., Lin, J. C.-H., Leary, R. J., Angenendt, P., Mankoo, P., Carter, H., Siu, I.-M., Gallia, G. L., Olivi, A., McLendon, R., Rasheed, B. A., Keir, S., Nikolskaya, T., Nikolsky, Y., Busam, D. A., Tekleab, H., Diaz, L. A., … Kinzler, K. W. (2008). An Integrated Genomic Analysis of Human Glioblastoma Multiforme. *Science*, *321*(5897), 1807–1812. https://doi.org/10.1126/science.1164382

Pasquier, B., Pasquier, D., N'golet, A., Panh, M. H., & Couderc, P. (1980). Extraneural metastases of astrocytomas and glioblastomas clinicopathological study of two cases and review of literature.

Cancer, *45*(1), 112–125. https://doi.org/10.1002/1097-0142(19800101)45:1<112::AID-CNCR2820450121>3.0.CO;2-9

Paulson, H. L., Das, S. S., Crino, P. B., Perez, M. K., Patel, S. C., Gotsdiner, D., Fischbeck, K. H., & Pittman, R. N. (1997). Machado-Joseph disease gene product is a cytoplasmic protein widely expressed in brain. *Annals of Neurology*, *41*(4), 453–462. https://doi.org/10.1002/ana.410410408

Pfoh, R., Lacdao, I. K., & Saridakis, V. (2015). Deubiquitinases and the new therapeutic opportunities offered to cancer. *Endocrine-Related Cancer*, *22*(1), T35–T54. https://doi.org/10.1530/ERC-14-0516

Phillips, H. S., Kharbanda, S., Chen, R., Forrest, W. F., Soriano, R. H., Wu, T. D., Misra, A., Nigro, J. M., Colman, H., Soroceanu, L., Williams, P. M., Modrusan, Z., Feuerstein, B. G., & Aldape, K. (2006). Molecular subclasses of high-grade glioma predict prognosis, delineate a pattern of disease progression, and resemble stages in neurogenesis. *Cancer Cell*, *9*(3), 157–173. https://doi.org/10.1016/j.ccr.2006.02.019

Pojo, M., Gonçalves, C. S., Xavier-Magalhães, A., Oliveira, A. I., Gonçalves, T., Correia, S., Rodrigues, A. J., Costa, S., Pinto, L., Pinto, A. A., Lopes, J. M., Reis, R. M., Rocha, M., Sousa, N., & Costa, B. M. (2015). A transcriptomic signature mediated by HOXA9 promotes human glioblastoma initiation, aggressiveness and resistance to temozolomide. *Oncotarget*, *6*(10), 7657–7674. https://doi.org/10.18632/oncotarget.3150

Porta, C., Paglino, C., & Mosca, A. (2014). Targeting PI3K/Akt/mTOR Signaling in Cancer. *Frontiers in Oncology*, *4*. https://doi.org/10.3389/fonc.2014.00064

Preston, D. L., Ron, E., Tokuoka, S., Funamoto, S., Nishi, N., Soda, M., Mabuchi, K., & Kodama, K. (2007). Solid cancer incidence in atomic bomb survivors: 1958-1998. *Radiation Research*, *168*(1), 1–64. https://doi.org/10.1667/RR0763.1

Qin, S., Wang, M., Zhang, T., & Zhang, S. (2014). Vitamin e intake is not associated with glioma risk: Evidence from a meta-analysis. *Neuroepidemiology*, *43*(3–4), 253–258. https://doi.org/10.1159/000369345

Ranum, L. P. W., Lundgren, J. K., Schut, L. J., Ahrens, M. J., Perlman, S., Aita, J., Bird, T. D., Gomez, C., & Orr, H. T. (1995). Spinocerebellar ataxia type 1 and Machado-Joseph disease: Incidence of CAG expansions among adult-onset ataxia patients from 311 families with dominant, recessive, or sporadic ataxia. *American Journal of Human Genetics*, *57*(3), 603–608.

Ray, S. K. (2016). The Transcription Regulator Kruppel-Like Factor 4 and Its Dual Roles of Oncogene in Glioblastoma and Tumor Suppressor in Neuroblastoma. *Forum on Immunopathological Diseases and Therapeutics*, *7*(1–2), 127–139. https://doi.org/10.1615/ForumImmunDisTher.2016017227

Reitman, Z. J., & Yan, H. (2010). Isocitrate dehydrogenase 1 and 2 mutations in cancer: Alterations at a crossroads of cellular metabolism. *Journal of the National Cancer Institute*, *102*(13), 932–941. https://doi.org/10.1093/jnci/djq187

Riemenschneider, M. J., & Reifenberger, G. (2009). Molecular neuropathology of gliomas. *International Journal of Molecular Sciences*, *10*(1), 184–212. https://doi.org/10.3390/ijms10010184

Rodrigues, A.-J., Coppola, G., Santos, C., Costa, M. do C., Ailion, M., Sequeiros, J., Geschwind, D. H., & Mariel, P. (2007). Functional genomics and biochemical characterization of the C. elegans

orthologue of the Machado-Joseph disease protein ataxin-3 . *The FASEB Journal*, *21*(4), 1126–1136. https://doi.org/10.1096/fj.06-7002com

Rodrigues, A. J., do Carmo Costa, M., Silva, T. L., Ferreira, D., Bajanca, F., Logarinho, E., & Maciel, P. (2010). Absence of ataxin-3 leads to cytoskeletal disorganization and increased cell death. *Biochimica et Biophysica Acta - Molecular Cell Research*, *1803*(10), 1154–1163. https://doi.org/10.1016/j.bbamcr.2010.07.004

Rodríguez-Lebrón, E., Costa, M. D., Luna-Cancalon, K., Peron, T. M., Fischer, S., Boudreau, R. L., Davidson, B. L., & Paulson, H. L. (2013). Silencing mutant ATXN3 expression resolves molecular phenotypes in SCA3 transgenic mice. *Molecular Therapy*, *21*(10), 1909–1918. https://doi.org/10.1038/mt.2013.152

Rosen, J., Blau, T., Grau, S. J., Barbe, M. T., Fink, G. R., & Galldiks, N. (2018). Extracranial Metastases of a Cerebral Glioblastoma: A Case Report and Review of the Literature. *Case Reports in Oncology*, *11*(2), 591–600. https://doi.org/10.1159/000492111

Sacco, J. J., Yau, T. Y., Darling, S., Patel, V., Liu, H., Urbé, S., Clague, M. J., & Coulson, J. M. (2014). The deubiquitylase Ataxin-3 restricts PTEN transcription in lung cancer cells. *Oncogene*, *33*(33), 4265–4272. https://doi.org/10.1038/onc.2013.512

Sadetzki, S., Chetrit, A., Freedman, L., Stovall, M., Modan, B., & Novikov, I. (2005). Long-term follow-up for brain tumor development after childhood exposure to ionizing radiation for tinea capitis. *Radiation Research*, *164*(2), 234. https://doi.org/10.1667/0033-7587(2005)164[0234:E]2.0.CO;2

Scheel, H., Tomiuk, S., & Hofmann, K. (2003). Elucidation of ataxin-3 and ataxin-7 function by integrative bioinformatics. *Human Molecular Genetics*, *12*(21), 2845–2852. https://doi.org/10.1093/hmg/ddg297

Schmitt, I., Brattig, T., Gossen, M., & Riess, O. (1997). Characterization of the rat spinocerebellar ataxia type 3 gene. *Neurogenetics*, *1*(2), 103–112. https://doi.org/10.1007/s100480050015

Schoemaker, M. J., Swerdlow, A. J., Hepworth, S. J., McKinney, P. A., Van Tongeren, M., & Muir, K. R. (2006). History of allergies and risk of glioma in adults. *International Journal of Cancer*, *119*(9), 2165–2172. https://doi.org/10.1002/ijc.22091

Schwartzbaum, J., Ding, B., Johannesen, T. B., Osnes, L. T. N., Karavodin, L., Ahlbom, A., Feychting, M., & Grimsrud, T. K. (2012). Association between prediagnostic IgE levels and risk of glioma. *Journal of the National Cancer Institute*, *104*(16), 1251–1259. https://doi.org/10.1093/jnci/djs315

Schweitzer, T., Vince, G., Herbold, C., Roosen, K., & Tonn, C. (2001). Extraneural metastases of primary brain tumors. *J Neurooncol*, *53*(2), 107–114. https://doi.org/10.1023/a:1012245115209.

Seo, Y. J., Cho, W. H., Kang, D. W., & Cha, S. H. (2012). Extraneural metastasis of glioblastoma multiforme presenting as an unusual neck mass. *Journal of Korean Neurosurgical Society*, *51*(3), 147–150. https://doi.org/10.3340/jkns.2012.51.3.147

Shao, C., Zhao, W., Qi, Z., & He, J. (2016). Smoking and glioma risk: Evidence from a meta-analysis of 25 observational studies. *Medicine (United States)*, *95*(2), 1–9. https://doi.org/10.1097/MD.0000000000002447

Shi, Z., Chen, J., Zhang, X., Chu, J., Han, Z., Xu, D., Gan, S., Pan, X., Ye, J., & Cui, X. (2018). Ataxin-3 promotes testicular cancer cell proliferation by inhibiting anti-oncogene PTEN. *Biochemical and*

Biophysical Research Communications, *503*(1), 391–396. https://doi.org/10.1016/j.bbrc.2018.06.047

Silva-Fernandes, A., Duarte-Silva, S., Neves-Carvalho, A., Amorim, M., Soares-Cunha, C., Oliveira, P., Thirstrup, K., Teixeira-Castro, A., & Maciel, P. (2014). Chronic Treatment with 17-DMAG Improves Balance and Coordination in A New Mouse Model of Machado-Joseph Disease. *Neurotherapeutics*, *11*(2), 433–449. https://doi.org/10.1007/s13311-013-0255-9

Simpson, J. R., Horton, J., Scott, C., Curran, W. J., Rubin, P., Fischbach, J., Isaacson, S., Rotman, M., Asbell, S. O., Nelson, J. S., Weinstein, A. S., & Nelson, D. F. (1993). Influence of location and extent of surgical resection on survival of patients with glioblastoma multiforme: Results of three consecutive radiation therapy oncology group (RTOG) clinical trials. *International Journal of Radiation Oncology, Biology, Physics*, *26*(2), 239–244. https://doi.org/10.1016/0360-3016(93)90203-8

Smith, C., & Ironside, J. W. (2007). Diagnosis and pathogenesis of gliomas. *Current Diagnostic Pathology*, *13*(3), 180–192. https://doi.org/10.1016/j.cdip.2007.04.002

Smith, J. S., Perry, A., Borell, T. J., Lee, H. K., O'Fallon, J., Hosek, S. M., Kimmel, D., Yates, A., Burger, P. C., Scheithauer, B. W., & Jenkins, R. B. (2000). Alterations of Chromosome Arms 1p and 19q as Predictors of Survival in Oligodendrogliomas, Astrocytomas, and Mixed Oligoastrocytomas. *Journal of Clinical Oncology*, *18*(3), 636–636. https://doi.org/10.1200/JCO.2000.18.3.636

So, J. S., Kim, H., & Han, K. S. (2021). Mechanisms of Invasion in Glioblastoma: Extracellular Matrix, Ca2+ Signaling, and Glutamate. *Frontiers in Cellular Neuroscience*, *15*(June), 1–10. https://doi.org/10.3389/fncel.2021.663092

Song, A., Wu, Y., Chu, W., Yang, X., Zhu, Z., Yan, E., Zhang, W., Zhou, J., Ding, X., Liu, J., Zhu, H., Ye, J., Wu, Y., Zheng, Y., & Song, X. (2021). Involvement of miR-619-5p in resistance to cisplatin by regulating ATXN3 in oral squamous cell carcinoma. *International Journal of Biological Sciences*, *17*(2), 430–447. https://doi.org/10.7150/ijbs.54014

Sonoda, Y., Ozawa, T., Hirose, Y., Aldape, K. D., McMahon, M., Berger, M. S., & Pieper, R. O. (2001). Formation of Intracranial Tumors by Genetically Modified Human Astrocytes Defines Four Pathways Critical in the Development of Human Anaplastic Astrocytoma. *Cancer Res.*, *61*(13), 4956–4960.

Strobel, H., Baisch, T., Fitzel, R., Schilberg, K., Siegelin, M. D., Karpel-Massler, G., Debatin, K.-M., & Westhoff, M.-A. (2019). Temozolomide and Other Alkylating Agents in Glioblastoma Therapy. *Biomedicines*, *7*(3), 69. https://doi.org/10.3390/biomedicines7030069

Stupp, R., Hegi, M. E., Mason, W. P., van den Bent, M. J., Taphoorn, M. J., Janzer, R. C., Ludwin, S. K., Allgeier, A., Fisher, B., Belanger, K., Hau, P., Brandes, A. A., Gijtenbeek, J., Marosi, C., Vecht, C. J., Mokhtari, K., Wesseling, P., Villa, S., Eisenhauer, E., … Mirimanoff, R. O. (2009). Effects of radiotherapy with concomitant and adjuvant temozolomide versus radiotherapy alone on survival in glioblastoma in a randomised phase III study: 5-year analysis of the EORTC-NCIC trial. *The Lancet Oncology*, *10*(5), 459–466. https://doi.org/10.1016/S1470-2045(09)70025-7

Stupp, R., Hegi, M. E., van den Bent, M. J., Mason, W. P., Weller, M., Mirimanoff, R. O., & Cairncross, J. G. (2006). Changing Paradigms—An Update on the Multidisciplinary Management of Malignant Glioma. *The Oncologist*, *11*(2), 165–180. https://doi.org/10.1634/theoncologist.11-2-165

Stupp, R., Mason, W. P., Van Den Bent, M. J., Weller, M., Fisher, B., Taphoorn, M. J. B., Belanger, K., Brandes, A. A., Marosi, C., Bogdahn, U., Curschmann, J., Janzer, R. C., Ludwin, S. K., Gorlia, T.,

Allgeier, A., Lacombe, D., Cairncross, J. G., Eisenhauer, E., & Mirimanoff, R. O. (2005). Radiotherapy plus Concomitant and Adjuvant Temozolomide for Glioblastoma. *N Engl J Med*, *10*(352), 987–996. www.nejm.org

Sung, H., Ferlay, J., Siegel, R. L., Laversanne, M., Soerjomataram, I., Jemal, A., & Bray, F. (2021). Global cancer statistics 2020: GLOBOCAN estimates of incidence and mortality worldwide for 36 cancers in 185 countries. *CA: A Cancer Journal for Clinicians*, *0*(0), 1–41. https://doi.org/10.3322/caac.21660

Svien, H. J., & Mabon, R. F. (1949). A simplified classification of the gliomas, based on the concept of anaplasia. *The Surgical Clinics of North America*, *29*(4), 1169–1187. https://doi.org/10.1016/S0039-6109(16)32797-9

Szopa, W., Burley, T. A., Kramer-Marek, G., & Kaspera, W. (2017). Diagnostic and therapeutic biomarkers in glioblastoma: Current status and future perspectives. *BioMed Research International*, *2017*. https://doi.org/10.1155/2017/8013575

Tait, D., Riccio, M., Sittler, A., Scherzinger, E., Santi, S., Ognibene, A., Maraldi, N. M., Lehrach, H., & Wanker, E. E. (1998). Ataxin-3 is transported into the nucleus and associates with the nuclear matrix. *Human Molecular Genetics*, *7*(6), 991–997. https://doi.org/10.1093/hmg/7.6.991

Takiyama, Y., Nishizawa, M., Tanaka, H., Kawashima, S., Sakamoto, H., Karube, Y., Shimazaki, H., Soutome, M., Endo, K., Ohta, S., Kagawa, Y., Kanazawa, I., Mizuno, Y., Yoshida, M., Yuasa, T., Horikawa, Y., Oyanagi, K., Nagai, H., Kondo, T., … Tsuji, S. (1993). The gene for Machado-Joseph disease maps to human chromosome 14q. *Nature Genetics*, *4*, 300–304. https://doi.org/https://doi.org/10.1038/ng0793-300

Taylor, O. G., Brzozowski, J. S., & Skelding, K. A. (2019). Glioblastoma multiforme: An overview of emerging therapeutic targets. *Frontiers in Oncology*, *9*(SEP), 1–11. https://doi.org/10.3389/fonc.2019.00963

The Cancer Genome Atlas Research Network. (2008). Comprehensive genomic characterization defines human glioblastoma genes and core pathways. *Nature*, *455*(7216), 1061–1068. https://doi.org/10.1038/nature07385

Todi, S. V., Scaglione, K. M., Blount, J. R., Basrur, V., Conlon, K. P., Pastore, A., Elenitoba-Johnson, K., & Paulson, H. L. (2010). Activity and cellular functions of the deubiquitinating enzyme and polyglutamine disease protein ataxin-3 are regulated by ubiquitination at lysine 117. *Journal of Biological Chemistry*, *285*(50), 39303–39313. https://doi.org/10.1074/jbc.M110.181610

Todi, S. V., Winborn, B. J., Scaglione, K. M., Blount, J. R., Travis, S. M., & Paulson, H. L. (2009). Ubiquitination directly enhances activity of the deubiquitinating enzyme ataxin-3. *EMBO Journal*, *28*(4), 372–382. https://doi.org/10.1038/emboj.2008.289

Trottier, Y., An-gourfinkel, I., Lutz, Y., Weber, C., Brice, A., Hirsch, E., & Mandel, J. (1998). Heterogeneous Intracellular Localization and Expression of Ataxin-3. *Neurobiology of Disease*, *347*, 335–347.

Tsuruga, Y., Kiyono, T., Matsushita, M., Takahashi, T., Kasai, H., Matsumoto, S., & Todo, S. (2008). Establishment of immortalized human hepatocytes by introduction of HPV16 E6/E7 and hTERT as cell sources for liver cell-based therapy. *Cell Transplantation*, *17*(9), 1083–1094. http://www.ncbi.nlm.nih.gov/pubmed/19177844

Turkalp, Z., Karamchandani, J., & Das, S. (2014). IDH mutation in glioma: New insights and promises for the future. *JAMA Neurology*, *71*(10), 1319–1325.

https://doi.org/10.1001/jamaneurol.2014.1205

Vital, A. L., Tabernero, M. D., Castrillo, A., Rebelo, O., Tão, H., Gomes, F., Nieto, A. B., Oliveira, C. R., Lopes, M. C., & Orfao, A. (2010). Gene expression profiles of human glioblastomas are associated with both tumor cytogenetics and histopathology. *Neuro-Oncology*, *12*(9), 991–1003. https://doi.org/10.1093/neuonc/noq050

Vogelstein, B., & Kinzler, K. W. (2004). Cancer genes and the pathways they control. *Nature Medicine*, *10*(8), 789–799. https://doi.org/10.1038/nm1087

Walsh, K. M., Ohgaki, H., & Wrensch, M. R. (2016). Epidemiology. *Handbook of Clinical Neurology*, *134*, 3–18. https://doi.org/10.1016/B978-0-12-802997-8.00001-3

Weishäupl, D., Schneider, J., Pinheiro, B. P., Ruess, C., Dold, S. M., von Zweydorf, F., Johannes Gloeckner, C., Schmidt, J., Riess, O., & Schmidt, T. (2019). Physiological and pathophysiological characteristics of ataxin-3 isoforms. *Journal of Biological Chemistry*, *294*(2), 644–661. https://doi.org/10.1074/jbc.RA118.005801

Weller, M., Wick, W., Aldape, K., Brada, M., Berger, M., Pfister, S. M., Nishikawa, R., Rosenthal, M., Wen, P. Y., Stupp, R., & Reifenberger, G. (2015). Glioma. *Nature Reviews Disease Primers*, *1*(July). https://doi.org/10.1038/nrdp.2015.17

Wick, W., Weller, M., Van Den Bent, M., Sanson, M., Weiler, M., Von Deimling, A., Plass, C., Hegi, M., Platten, M., & Reifenberger, G. (2014). MGMT testing - The challenges for biomarker-based glioma treatment. *Nature Reviews Neurology*, *10*(7), 372–385. https://doi.org/10.1038/nrneurol.2014.100

Wiemels, J. L., Wiencke, J. K., Sison, J. D., Miike, R., McMillan, A., & Wrensch, M. (2002). History of allergies among adults with glioma and controls. *International Journal of Cancer*, *98*(4), 609–615. https://doi.org/10.1002/ijc.10239

Wilson, T. A., Karajannis, M. A., & Harter, D. H. (2014). Glioblastoma multiforme: State of the art and future therapeutics. *Surgical Neurology International*, *5*(Supplement). https://doi.org/10.4103/2152-7806.132138

Winborn, B. J., Travis, S. M., Todi, S. V., Scaglione, K. M., Xu, P., Williams, A. J., Cohen, R. E., Peng, J., & Paulson, H. L. (2008). The deubiquitinating enzyme ataxin-3, a polyglutamine disease protein, edits Lys63 linkages in mixed linkage ubiquitin chains. *Journal of Biological Chemistry*, *283*(39), 26436–26443. https://doi.org/10.1074/jbc.M803692200

Wirsching, H. G., Galanis, E., & Weller, M. (2016). Glioblastoma. *Handbook of Clinical Neurology*, *134*, 381–397. https://doi.org/10.1016/B978-0-12-802997-8.00023-2

Xavier-Magalhães, A., Nandhabalan, M., Jones, C., & Costa, B. M. (2013). Molecular prognostic factors in glioblastoma: state of the art and future challenges. *CNS Oncology*, *2*(6), 495–510. https://doi.org/10.2217/cns.13.48

Yan, H., Parsons, D. W., Jin, G., McLendon, R., Rasheed, B. A., Yuan, W., Kos, I., Batinic-Haberle, I., Jones, S., Riggins, G. J., Friedman, H., Friedman, A., Reardon, D., Herndon, J., Kinzler, K. W., Velculescu, V. E., Vogelstein, B., & Bigner, D. D. (2009). IDH1 and IDH2 Mutations in Gliomas. *New England Journal of Medicine*, *360*(8), 765–773. https://doi.org/10.1056/NEJMoa0808710

Zeng, L. X., Tang, Y., & Ma, Y. (2014). Ataxin-3 expression correlates with the clinicopathologic features of gastric cancer. *International Journal of Clinical and Experimental Medicine*, *7*(4), 973–981.

Zhang, J., F.G. Stevens, M., & D. Bradshaw, T. (2012). Temozolomide: Mechanisms of Action, Repair

and Resistance. *Current Molecular Pharmacology*, *5*(1), 102–114. https://doi.org/10.2174/1874-470211205010102

Zhang, Y., Dube, C., Gibert, M., Cruickshanks, N., Wang, B., Coughlan, M., Yang, Y., Setiady, I., Deveau, C., Saoud, K., Grello, C., Oxford, M., Yuan, F., & Abounader, R. (2018). The p53 pathway in glioblastoma. *Cancers*, *10*(9). https://doi.org/10.3390/cancers10090297

Zou, H., Chen, H., Zhou, Z., Wan, Y., & Liu, Z. (2019). ATXN3 promotes breast cancer metastasis by deubiquitinating KLF4. *Cancer Letters*, *467*(September), 19–28. https://doi.org/10.1016/j.canlet.2019.09.012